cells line were cultured in Dulbecco's modified Eagle's medium (DMEM) supplemented with 10% heat-inactivated fetal bovine serum (FBS) and antibiotics. The P19 murine teratocarcinoma cell line was cultured in α-modified Eagle's medium supplemented with 10% FBS and antibiotics. Twist-1-overexpressing MC3T3-E1 (MC3T3-E1-Tw1) cells were obtained by puromycin selection of MC3T3-E1 cells transfected with pCAGIP-Flag-Twist-1. Screening of Twist-1-overexpressing clones was performed by western blotting of immunoprecipitates using anti-Flag antibody.

siRNA method

Target short interfering RNA (siRNA) was determined using the siRNA design tool (Invitrogen). The siTwist-604 sense sequence was 5′-AAGCUGAGCAAGAUUCAGACC-3′; siTwist-691 sense sequence was 5′-AAGAUGGCAAGCUGCAGCUAU-3′; siTwist-645 sense sequence was 5′-CAUCGACUUCCUGUACCAGGU-3′; and siTwist-481 sense sequence was 5′-CAGUCGUACGAGGAGCUGCAG-3′. As a control, the non-silencing siRNA sense sequence was 5′-AAGCGCGCUUUGUAGGAUUCG-3′. C3H10T1/2 cells were seeded at 70% confluence on the day before transfection. Transfections were performed using Lipofectamine 2000 transfection reagent (Invitrogen). To examine the effects of Twist-1-specific siRNA on reporter constructs, cells were transfected with 3GC2-Lux and pRL-TK vector (Promega, Madison, WI) using FuGENE6 transfection reagent (Roche, Basel, Switzerland) 24 hours after siRNA transfection. At 36 hours after siRNA transfection, cells were treated with rhBMP2 (300 ng/ml) for 12 hours. Both firefly and *Renilla* luciferase activities were measured 2 days after siRNA transfection using a dual luciferase assay system (Promega). Co-transfections of siRNA and plasmid DNAs were performed using X-treamGENE siRNA transfection reagent (Roche).

RNA extraction and northern blot analysis

Total RNA was isolated using Isogen (Nippon Gene, Tokyo, Japan) according to the instructions of the manufacturer. Total RNA (15 μg) was denatured, electrophoresed in 2% agarose gels containing 18% formaldehyde, then transferred to Hybond-N+ membrane (Amersham Biosciences, Piscataway, NJ). Membranes were hybridized at 65°C for 12 hours in a hybridization buffer, PerfectHyb (Toyobo, Osaka Japan). Probes for Twist-1, osteocalcin, osteopontin and G3PDH were labeled using the RadPrime DNA labeling system (Invitrogen). After hybridization, membranes were washed four times with 2× standard sodium citrate (SSC) and 0.1% sodium dodecyl sulfate (SDS). Blots were exposed to X-ray films using intensify screens at −80°C.

Alkaline phosphatase assay

Alkaline phosphatase (ALP) activity was assessed as previously described (Wakabayashi et al., 2002). Briefly, cell lysates were centrifuged and supernatants were used for enzyme assays. ALP activity was measured according to the methods of Kind-King, using a test kit (Wako, Osaka, Japan) with phenylphosphate as a substrate. Enzyme activity was expressed in King-Armstrong (K-A) units, normalized to protein concentration. Results are presented as mean ± standard deviation (s.d.) from a representative experiment. Statistical analysis was performed using analysis of variance (ANOVA).

Transfections and reporter assays

P19 cells were transiently transfected using 3GC2-Lux together with expression constructs of Smad1, Smad4, Twist-1, E47, Id1 and BMPR-IB(QD) using FuGENE6 transfection reagent. P19 cells were chosen because the cells responded to BMPs and expressed some of the BMP target genes. Additionally, transfection efficiency was higher in P19 cells than in other cell lines. At 24 hours after transfection, both firefly and *Renilla* luciferase activities were assayed with the dual luciferase assay system (Promega) using a Lumat LB 9507 luminometer (Berthold Technologies, Wildbad, Germany). Firefly luciferase activity was normalized with respect to *Renilla* luciferase activity. All assays were performed at least three times in duplicate or triplicate. Results are presented as mean ± s.d. from a representative experiment. Statistical analysis was performed using ANOVA.

Immunoprecipitation and immunoblotting

COS-7 cells were transiently transfected with the expression construct using FuGENE6 transfection reagent. COS-7 cells were used because they contained no endogenous Twist-1. At 24 hours after transfection, cells were lysed in buffer containing 25 mM Hepes pH 8.0, 150 mM KCl, 2 mM EDTA, 0.1% Nonidet P-40 (NP-40) and EDTA-free complete protease inhibitor cocktail (Roche). After 20 minutes on ice, cell lysates were pelleted by centrifugation and supernatants were pre-cleared with normal mouse IgG (Santa Cruz, Santa Cruz, CA) for 30 minutes at 4°C, then incubated with anti-FLAG M2 affinity gel (Sigma, St Louis, MO) for 4 hours at 4°C. Immunoprecipitates were washed four times with the buffer used for cell solubilization. Immune complexes were eluted at 98°C for 5 minutes in Laemmli's sample buffer. Immunoprecipitates were separated by SDS-polyacrylamide gel electrophoresis (PAGE), transferred to polyvilinidendifluoride (PVDF) membrane, and immunoblotted with anti-Flag M2 antibody (Sigma) and anti-Myc antibody (MBL, Nagoya Japan). Protein bands were visualized using Chemi-Lumi One (Nacalai Tesque, Kyoto, Japan).

To detect overexpressed Smad1 and Smad4, P19 cells were lysed as described above, 24 hours after transfection. Lysates were separated by SDS-PAGE, transferred to PVDF membrane, and immunoblotted with anti-Smad1 and -Smad4 antibody (Santa Cruz) and anti-β-actin antibody (ABcam, Cambrige, UK). Protein bands were visualized using Chemi-Lumi One (Nacalai Tesque).

Nuclear protein extracts were prepared from MC3T3-E1 cells as follows. Cells were harvested by centrifugation at 500 ***g*** for 10 minutes at 4°C. Cell pellets were washed by gentle resuspension in cold PBS-0.5 mM EDTA and nuclei isolation buffer (NIB) containing 10 mM Tris-HCl (pH 7.5), 60 mM KCl, 15 mM NaCl, 1.5 mM $MgCl_2$, 1 mM $CaCl_2$, 0.25 M sucrose, 10% glycerol, 0.1 mM phenylmethylsulfonylfluoride (PMSF) and EDTA-free complete protease inhibitor cocktail (Roche). Cells were re-suspended with ice-cold NIB containing 0.1% NP-40 and allowed to swell for 10 minutes on ice. Swollen cells were centrifuged at 500 ***g*** for 10 minutes at 4°C. Nuclei pellets were washed in cold NIB and centrifuged at 500 ***g*** for 5 minutes at 4°C. Nuclear pellets were diluted to 1.5 mg/ml DNA with ice-cold NIB and digested using micrococcal nuclease (80 units/mg DNA; Worthington, Lakewood, NJ). Digested nuclei were rapidly cooled on ice for 10 minutes and centrifuge at 12,800 ***g*** for 10 minutes at 4°C. Supernatant (S1) was collected and pellets were re-suspended with ice-cold cell lysis buffer containing 10 mM Tris-HCl (pH 7.5), 2 mM EDTA, 10% glycerol, 300 mM NaCl, 0.1 mM PMSF and EDTA-free complete protease inhibitor cocktail (Roche), then incubated for 45 minutes on ice. Nuclear debris was spun out by centrifugation at 12,800 ***g*** for 10 minutes at 4°C, and the supernatant (S2) was collected. S1 and S2 fractions were combined, then incubated with anti-Flag M2 affinity gel (Sigma) for 4 hours at 4°C. Immunoprecipitates were washed four times with cell lysis buffer containing 0.1% NP-40. Immune complexes were eluted at 98°C for 5 minutes in Laemmli's sample buffer. Immunoprecipitates were separated by SDS-PAGE, transferred to PVDF membrane, and immunoblotted using anti-Flag M2 antibody (Sigma).

To analyze the interaction of Id1 and E47, or Smad4, HDAC1 and Flag-Twist-1, C3H10T1/2 and MC3T3-E1-Tw1 cells were lysed with RIPA buffer containing 50 mM Tris-HCl (pH 7.4), 1% NP-40, 0.25% sodium deoxycholate, 150 mM NaCl, 1 mM EDTA and EDTA-free complete protease inhibitor cocktail (Roche), and the supernatant was obtained by centrifugation of the lysates at 12,800 ***g*** for 5 minutes at 4°C. After the removal of non-specifically bound substances using non-immune IgG (Santa Cruz), the supernatant was incubated with anti-E47 (Santa Cruz) antibody for 2 hours at 4°C and precipitated with protein A beads, or anti-Flag M2 affinity gel for 4 hours at 4°C. After washing the precipitates four times with the RIPA buffer, immune complexes were eluted at 98°C for 5 minutes in Laemmli's sample buffer. Immunoprecipitates were separated by SDS-PAGE, transferred to PVDF membrane, and immunoblotted using anti-Id1, anti-Smad4 (Santa Cruz), anti-Smad1 (Zymed, San Francisco, CA), anti-HDAC1(Upstate Temecula, CA) antibodies.

Pulse-chase assay

Pulse-chase assay was performed according to the method previously described (Deed et al., 1996), with minor modification. COS-7 cells were transfected with Flag-Twist-1, Myc-E47 and Myc-Id1 using FuGENE6 transfection reagent. At 24 hours after transfection, cells were starved in cysteine and methionine-free DMEM (Invitrogen) containing with 5% dialyzed FBS for 1 hour, then incubated for an additional 2 hours in cysteine and methionine-free DMEM containing 10% dialyzed FBS and 50 μCi/ml of Promix (Amersham). Labeled cells were then incubated in standard DMEM supplemented with 10% FBS and harvested at various time points. Immunoprecipitation was performed as described above.

Real-time quantitative PCR

MC3T3-E1-Tw1 cells (2×10^5 cells) were treated with BMP (600 ng) alone or the mixture of BMP (600 ng) and trichostatin (TSA, 330 nM; Sigma). At 24 hours after the treatment, total RNA was extracted from cells using RNeasy kits (Qiagen, Hilden, Germany) and digested with DNase I according to the manufacturer's instructions. Total RNA (5 μg) was reverse transcribed into cDNA using High Capacity cDNA Archive Kits (Applied Biosystems, Foster City, CA) and amplified by real-time quantitative PCR using an ABI PRISM 7700 Sequence Detection System (Applied Biosystems, Foster City, CA). Mixtures of probes and primer pairs specific for murine ALP, Runx2, osteopontin and GAPDH were purchased from Applied Biosystems (Foster City, CA). The concentration of target genes was determined using the comparative CT method (threshold cycle number at the cross-point between amplification plot and threshold) and values were normalized to an internal GAPDH control. Results are presented as mean ± s.d. from a representative experiment.

We wish to thank K. Miyazono for providing the 3GC2-Lux luciferase construct, BMPR-IB(QD) and TβR-I(TD), and Astellas Pharmaceutical Co. for providing rhBMP2. This work was supported by the Northern Osaka (Saito) Biomedical Knowledge-Based Cluster Creation Project, a Grant-in-Aid from the Ministry of Education,

Culture, Sports, Science and Technology, the Japanese Government, and Takeda Science Foundation.

References

Benezra, R., Davis, R. L., Lockshon, D., Turner, D. L. and Weintraub, H. (1990). The protein Id: a negative regulator of helix-loop-helix DNA binding proteins. *Cell* **61**, 49-59.

Bialek, P., Kern, B., Yang, X., Schrock, M., Sosic, D., Hong, N., Wu, H., Yu, K., Ornitz, D. M., Olson, E. N. et al. (2004). A twist code determines the onset of osteoblast differentiation. *Dev. Cell* **6**, 423-435.

Bourgeois, P., Bolcato-Bellemin, A. L., Danse, J. M., Bloch-Zupan, A., Yoshiba, K., Stoetzel, C. and Perrin-Schmitt, F. (1998). The variable expressivity and incomplete penetrance of the twist-null heterozygous mouse phenotype resemble those of human Saethre-Chotzen syndrome. *Hum. Mol. Genet.* **7**, 945-957.

Centrella, M., Horowitz, M. C., Wozney, J. M. and McCarthy, T. L. (1994). Transforming growth factor-beta gene family members and bone. *Endocr. Rev.* **15**, 27-39.

Chen, Z. F. and Behringer, R. R. (1995). twist is required in head mesenchyme for cranial neural tube morphogenesis. *Genes Dev.* **9**, 686-699.

Deed, R. W., Armitage, S. and Norton, J. D. (1996). Nuclear localization and regulation of Id protein through an E protein-mediated chaperone mechanism. *J. Biol. Chem.* **271**, 23603-23606.

Derynck, R. and Zhang, Y. E. (2003). Smad-dependent and Smad-independent pathways in TGF-beta family signalling. *Nature* **425**, 577-584.

Ducy, P., Zhang, R., Geoffroy, V., Ridall, A. L. and Karsenty, G. (1997). Osf2/Cbfa1: a transcriptional activator of osteoblast differentiation. *Cell* **89**, 747-754.

El Ghouzzi, V., Legeai-Mallet, L., Aresta, S., Benoist, C., Munnich, A., de Gunzburg, J. and Bonaventure, J. (2000). Saethre-Chotzen mutations cause TWIST protein degradation or impaired nuclear location. *Hum. Mol. Genet.* **9**, 813-819.

Gong, X. Q. and Li, L. (2002). Dermo-1, a multifunctional basic helix-loop-helix protein, represses MyoD transactivation via the HLH domain, MEF2 interaction, and chromatin deacetylation. *J. Biol. Chem.* **277**, 12310-12317.

Hamamori, Y., Wu, H. Y., Sartorelli, V. and Kedes, L. (1997). The basic domain of myogenic basic helix-loop-helix (bHLH) proteins is the novel target for direct inhibition by another bHLH protein, Twist. *Mol. Cell. Biol.* **17**, 6563-6573.

Hamamori, Y., Sartorelli, V., Ogryzko, V., Puri, P. L., Wu, H. Y., Wang, J. Y., Nakatani, Y. and Kedes, L. (1999). Regulation of histone acetyltransferases p300 and PCAF by the bHLH protein twist and adenoviral oncoprotein E1A. *Cell* **96**, 405-413.

Harada, H., Tagashira, S., Fujiwara, M., Ogawa, S., Katsumata, T., Yamaguchi, A., Komori, T. and Nakatsuka, M. (1999). Cbfa1 isoforms exert functional differences in osteoblast differentiation. *J. Biol. Chem.* **274**, 6972-6978.

Hata, A., Lagna, G., Massague, J. and Hemmati-Brivanlou, A. (1998). Smad6 inhibits BMP/Smad1 signaling by specifically competing with the Smad4 tumor suppressor. *Genes Dev.* **12**, 186-197.

Hebrok, M., Fuchtbauer, A. and Fuchtbauer, E. M. (1997). Repression of muscle-specific gene activation by the murine Twist protein. *Exp. Cell Res.* **232**, 295-303.

Hogan, B. L. (1996). Bone morphogenetic proteins: multifunctional regulators of vertebrate development. *Genes Dev.* **10**, 1580-1594.

Hullinger, T. G., Pan, Q., Viswanathan, H. L. and Somerman, M. J. (2001). TGFbeta and BMP-2 activation of the OPN promoter: roles of smad- and hox-binding elements. *Exp. Cell Res.* **262**, 69-74.

Imamura, T., Takase, M., Nishihara, A., Oeda, E., Hanai, J., Kawabata, M. and Miyazono, K. (1997). Smad6 inhibits signalling by the TGF-beta superfamily. *Nature* **389**, 622-626.

Ishida, W., Hamamoto, T., Kusanagi, K., Yagi, K., Kawabata, M., Takehara, K., Sampath, T. K., Kato, M. and Miyazono, K. (2000). Smad6 is a Smad1/5-induced smad inhibitor. Characterization of bone morphogenetic protein-responsive element in the mouse Smad6 promoter. *J. Biol. Chem.* **275**, 6075-6079.

Ju, W., Hoffmann, A., Verschueren, K., Tylzanowski, P., Kaps, C., Gross, G. and Huylebroeck, D. (2000). The bone morphogenetic protein 2 signaling mediator Smad1 participates predominantly in osteogenic and not in chondrogenic differentiation in mesenchymal progenitors C3H10T1/2. *J. Bone Miner. Res.* **15**, 1889-1899.

Katagiri, T., Yamaguchi, A., Komaki, M., Abe, E., Takahashi, N., Ikeda, T., Rosen, V., Wozney, J. M., Fujisawa-Sehara, A. and Suda, T. (1994). Bone morphogenetic protein-2 converts the differentiation pathway of C2C12 myoblasts into the osteoblast lineage. *J. Cell Biol.* **127**, 1755-1766.

Lassar, A. B., Davis, R. L., Wright, W. E., Kadesch, T., Murre, C., Voronova, A., Baltimore, D. and Weintraub, H. (1991). Functional activity of myogenic HLH proteins requires hetero-oligomerization with E12/E47-like proteins in vivo. *Cell* **66**, 305-315.

Lee, K. S., Kim, H. J., Li, Q. L., Chi, X. Z., Ueta, C., Komori, T., Wozney, J. M., Kim, E. G., Choi, J. Y., Ryoo, H. M. et al. (2000). Runx2 is a common target of transforming growth factor beta1 and bone morphogenetic protein 2, and cooperation between Runx2 and Smad5 induces osteoblast-specific gene expression in the pluripotent mesenchymal precursor cell line C2C12. *Mol. Cell. Biol.* **20**, 8783-8792.

Lee, M. S., Lowe, G. N., Strong, D. D., Wergedal, J. E. and Glackin, C. A. (1999). TWIST, a basic helix-loop-helix transcription factor, can regulate the human osteogenic lineage. *J. Cell. Biochem.* **75**, 566-577.

Leptin, M. (1991). twist and snail as positive and negative regulators during Drosophila mesoderm development. *Genes Dev.* **5**, 1568-1576.

Li, L., Cserjesi, P. and Olson, E. N. (1995). Dermo-1: a novel twist-related bHLH protein expressed in the developing dermis. *Dev. Biol.* **172**, 280-292.

Liu, D., Black, B. L. and Derynck, R. (2001). TGF-beta inhibits muscle differentiation through functional repression of myogenic transcription factors by Smad3. *Genes Dev.* **15**, 2950-2966.

Massague, J. (2000). How cells read TGF-beta signals. *Nat. Rev. Mol. Cell Biol.* **1**, 169-178.

Murre, C., McCaw, P. S. and Baltimore, D. (1989). A new DNA binding and dimerization motif in immunoglobulin enhancer binding, daughterless, MyoD, and myc proteins. *Cell* **56**, 777-783.

Nakashima, K., Takizawa, T., Ochiai, W., Yanagisawa, M., Hisatsune, T., Nakafuku, M., Miyazono, K., Kishimoto, T., Kageyama, R. and Taga, T. (2001). BMP2-mediated alteration in the developmental pathway of fetal mouse brain cells from neurogenesis to astrocytogenesis. *Proc. Natl. Acad. Sci. USA* **98**, 5868-5873.

Niwa, H., Masui, S., Chambers, I., Smith, A. G. and Miyazaki, J. (2002). Phenotypic complementation establishes requirements for specific POU domain and generic transactivation function of Oct-3/4 in embryonic stem cells. *Mol. Cell. Biol.* **22**, 1526-1536.

Ogata, T., Wozney, J. M., Benezra, R. and Noda, M. (1993). Bone morphogenetic protein 2 transiently enhances expression of a gene, Id (inhibitor of differentiation), encoding a helix-loop-helix molecule in osteoblast-like cells. *Proc. Natl. Acad. Sci. USA* **90**, 9219-9222.

Peng, Y., Kang, Q., Luo, Q., Jiang, W., Si, W., Liu, B. A., Luu, H. H., Park, J. K., Li, X., Luo, J. et al. (2004). Inhibitor of DNA binding/differentiation helix-loop-helix proteins mediate bone morphogenetic protein-induced osteoblast differentiation of mesenchymal stem cells. *J. Biol. Chem.* **279**, 32941-32949.

Rice, D. P., Aberg, T., Chan, Y., Tang, Z., Kettunen, P. J., Pakarinen, L., Maxson, R. E. and Thesleff, I. (2000). Integration of FGF and TWIST in calvarial bone and suture development. *Development* **127**, 1845-1855.

Shi, X., Yang, X., Chen, D., Chang, Z. and Cao, X. (1999). Smad1 interacts with homeobox DNA-binding proteins in bone morphogenetic protein signaling. *J. Biol. Chem.* **274**, 13711-13717.

Spicer, D. B., Rhee, J., Cheung, W. L. and Lassar, A. B. (1996). Inhibition of myogenic bHLH and MEF2 transcription factors by the bHLH protein Twist. *Science* **272**, 1476-1480.

Sun, X. H. and Baltimore, D. (1991). An inhibitory domain of E12 transcription factor prevents DNA binding in E12 homodimers but not in E12 heterodimers. *Cell* **64**, 459-470.

Sun, X. H., Copeland, N. G., Jenkins, N. A. and Baltimore, D. (1991). Id proteins Id1 and Id2 selectively inhibit DNA binding by one class of helix-loop-helix proteins. *Mol. Cell. Biol.* **11**, 5603-5611.

Sun, Y., Nadal-Vicens, M., Misono, S., Lin, M. Z., Zubiaga, A., Hua, X., Fan, G. and Greenberg, M. E. (2001). Neurogenin promotes neurogenesis and inhibits glial differentiation by independent mechanisms. *Cell* **104**, 365-376.

Tamura, M. and Noda, M. (1999). Identification of DERMO-1 as a member of helix-loop-helix type transcription factors expressed in osteoblastic cells. *J. Cell. Biochem.* **72**, 167-176.

Thies, R. S., Bauduy, M., Ashton, B. A., Kurtzberg, L., Wozney, J. M. and Rosen, V. (1992). Recombinant human bone morphogenetic protein-2 induces osteoblastic differentiation in W-20-17 stromal cells. *Endocrinology* **130**, 1318-1324.

Thisse, B., el Messal, M. and Perrin-Schmitt, F. (1987). The twist gene: isolation of a Drosophila zygotic gene necessary for the establishment of dorsoventral pattern. *Nucleic Acids Res.* **15**, 3439-3453.

Urist, M. R. (1965). Bone: formation by autoinduction. *Science* **150**, 893-899.

Vinals, F. and Ventura, F. (2004). Myogenin protein stability is decreased by BMP-2 through a mechanism implicating Id1. *J. Biol. Chem.* **279**, 45766-45772.

Vinals, F., Reiriz, J., Ambrosio, S., Bartrons, R., Rosa, J. L. and Ventura, F. (2004). BMP-2 decreases Mash1 stability by increasing Id1 expression. *EMBO J.* **23**, 3527-3537.

Wakabayashi, S., Tsutsumimoto, T., Kawasaki, S., Kinoshita, T., Horiuchi, H. and Takaoka, K. (2002). Involvement of phosphodiesterase isozymes in osteoblastic differentiation. *J. Bone Miner. Res.* **17**, 249-256.

Wieser, R., Wrana, J. L. and Massague, J. (1995). GS domain mutations that constitutively activate T beta R-I, the downstream signaling component in the TGF-beta receptor complex. *EMBO J.* **14**, 2199-2208.

Wolf, C., Thisse, C., Stoetzel, C., Thisse, B., Gerlinger, P. and Perrin-Schmitt, F. (1991). The M-twist gene of Mus is expressed in subsets of mesodermal cells and is closely related to the Xenopus X-twi and the Drosophila twist genes. *Dev. Biol.* **143**, 363-373.

Wrana, J. L. (2000). Regulation of Smad activity. *Cell* **100**, 189-192.

Wrana, J. L., Attisano, L., Carcamo, J., Zentella, A., Doody, J., Laiho, M., Wang, X. F. and Massague, J. (1992). TGF beta signals through a heteromeric protein kinase receptor complex. *Cell* **71**, 1003-1014.

Yang, X., Ji, X., Shi, X. and Cao, X. (2000). Smad1 domains interacting with Hoxc-8 induce osteoblast differentiation. *J. Biol. Chem.* **275**, 1065-1072.

Yoshida, Y., Tanaka, S., Umemori, H., Minowa, O., Usui, M., Ikematsu, N., Hosoda, E., Imamura, T., Kuno, J., Yamashita, T. et al. (2000). Negative regulation of BMP/Smad signaling by Tob in osteoblasts. *Cell* **103**, 1085-1097.

Zhang, Y. W., Yasui, N., Ito, K., Huang, G., Fujii, M., Hanai, J., Nogami, H., Ochi, T., Miyazono, K. and Ito, Y. (2000). A RUNX2/PEBP2alpha A/CBFA1 mutation displaying impaired transactivation and Smad interaction in cleidocranial dysplasia. *Proc. Natl. Acad. Sci. USA* **97**, 10549-10554.

Available online at www.sciencedirect.com
ScienceDirect
Biochemical and Biophysical Research Communications 354 (2007) 453–458
BBRC
www.elsevier.com/locate/ybbrc

Bone marrow-derived osteoblast progenitor cells in circulating blood contribute to ectopic bone formation in mice

Satoru Otsuru [a,b], Katsuto Tamai [a,*], Takehiko Yamazaki [a], Hideki Yoshikawa [b], Yasufumi Kaneda [a]

[a] *Division of Gene Therapy Science, Osaka University Graduate School of Medicine, 2-2 Yamada-oka, Suita, Osaka 565-0871, Japan*
[b] *Department of Orthopaedic Surgery, Osaka University Graduate School of Medicine, 2-2 Yamada-oka, Suita, Osaka 565-0871, Japan*

Received 18 December 2006
Available online 10 January 2007

Abstract

Recent studies have suggested the existence of osteoblastic cells in the circulation, but the origin and role of these cells *in vivo* are not clear. Here, we examined how these cells contribute to osteogenesis in a bone morphogenetic protein (BMP)-induced model of ectopic bone formation. Following lethal dose-irradiation and subsequent green fluorescent protein-transgenic bone marrow cell-transplantation (GFP-BMT) in mice, a BMP-2-containing collagen pellet was implanted into muscle. Three weeks later, a significant number of GFP-positive osteoblastic cells were present in the newly generated ectopic bone. Moreover, peripheral blood mononuclear cells (PBMNCs) from the BMP-2-implanted mouse were then shown to include osteoblast progenitor cells (OPCs) in culture. Passive transfer of the PBMNCs isolated from the BMP-2-implanted GFP-mouse to the BMP-2-implanted nude mouse led to GFP-positive osteoblast accumulation in the ectopic bone. These data provide new insight into the mechanism of ectopic bone formation involving bone marrow-derived OPCs in circulating blood.

Keywords: Bone morphogenetic protein; Ectopic bone; Circulating osteoblast progenitor cells; Bone marrow transplantation

BMP-2 and other members of the BMP family are well-known inducers of bone formation *in vitro* and *in vivo* [1]. During healing of bone fractures, stimulation from BMPs recruits OPCs to the fracture sites and induces their differentiation to become osteoblasts. An experimental model of ectopic bone formation in mice has also indicated that BMP-2 stimulation is essential for the recruitment of OPCs to the osteogenic sites [2]. The source and the route for the recruitment of the OPCs in this model, however, have not been fully elucidated. Notably, the surrounding soft tissues, the periosteum and the bone marrow all constitute potential origins for the OPCs involved in osteogenesis, but it is unclear how these OPCs target the region expressing BMPs [3].

Recent studies have shown the existence of OPCs (or indeed osteoblasts) in the circulating blood of various mammals, including humans [4–6]. These reports indicate an ability of circulating cells to function as osteoblasts in culture and to form osseous tissues after transplantation, suggesting that OPCs and/or osteoblasts may be supplied via the circulation to regenerating bone *in vivo*. This hypothesis is potentially an attractive one for the field of bone-regenerative medicine, especially if an adequate number of circulating OPCs can be isolated from peripheral blood, expanded in culture, and delivered to sites requiring bone regeneration. However, the origins of circulating OPCs and evidence of endogenously circulating cells with the potential to migrate and contribute to bone regeneration *in vivo* have not yet been fully demonstrated.

Abbreviations: OPCs, osteoblast progenitor cells; BMPs, bone morphogenetic proteins; MOPCs, marrow-derived OPCs; GFP, green fluorescent protein; BMT, bone marrow transplantation; PBMNCs, peripheral blood mononuclear cells; DAPI, 6-diamidino-2-phenylindole; FITC, fluorescein isothiocyanate; H&E, hematoxylin and eosin; TRAP, tartrate-resistant acid phosphatise.

* Corresponding author. Fax: +81 6 6879 3909.
E-mail address: tamai@gts.med.osaka-u.ac.jp (K. Tamai).

0006-291X/$ - see front matter © 2007 Elsevier Inc. All rights reserved.
doi:10.1016/j.bbrc.2006.12.226

Here, we report for the first time that marrow-derived OPCs (MOPCs) can migrate to a BMP-2 pellet implanted into mouse muscle and differentiate to become osteoblasts within the BMP-2-induced ectopic bone. We have also succeeded in culturing circulating OPCs from PBMNCs isolated from BMP-2-implanted mice. Furthermore, intravenous transfer of the GFP-transgenic PBMNCs containing OPCs to nude mice implanted with BMP-2 pellet generates a significant number of GFP-osteoblasts in the BMP-2-induced ectopic bone. We believe that these new findings will accelerate further understanding of the role of circulating OPCs, not only in ectopic osteogenesis, but also in the healing of bone fractures *in vivo*.

Materials and methods

Bone marrow cell transplantation (BMT). Under sterile conditions, bone marrow cells were isolated from 8- to 10-week-old male C57BL/6 transgenic mice that ubiquitously expressed enhanced GFP [7]. Eight- to 10-week-old female C57BL/6 mice were lethally irradiated with 10 Gy. For BMT, each irradiated mouse received 5×10^6 bone marrow cells from GFP transgenic mice. Experiments on BMT mice were performed at least 6 weeks after BMT. All animals were handled according to approved protocols and the guidelines of the Animal Committee of Osaka University.

Preparation and implantation of BMP-2-containing collagen pellets. Recombinant human BMP-2 was provided by Astellas Pharma Inc. (Tokyo, Japan). The BMP-2 was suspended in buffer solution (5 mmol/L glutamic acid, 2.5% glycine, 0.5% sucrose, and 0.01% Tween 80) at a concentration of 1 μg/μL. Next, 3 μL (3 μg of BMP-2) of the BMP-2 solution was diluted in 22 μL PBS and blotted onto a porous collagen disc (6 mm diameter, 1 mm thickness), freeze-dried, and stored at −20 °C. All procedures were carried out under sterile conditions. BMP-2-containing or control PBS-containing collagen pellets were implanted onto the backs (below muscle fascia) of BMT mice, C57BL/6 mice, or nude mice. Three weeks later, fluorescent photos of ectopic bone formation were taken using a digital microscope (Multiviewer system VB-S20 KEYENCE, Osaka, Japan).

Morphological and immunofluorescent analysis of the ectopic bone. Ectopic bone was removed and fixed with 4% paraformaldehyde at 4 °C for 48 h. After taking soft X-ray photos, the bones were decalcified at 4 °C for 6 days with the EDTA solution replaced every other day. After decalcification, the pellets were equilibrated in PBS containing 15% sucrose for 12 h and then in PBS containing 30% sucrose for 12 h, embedded in Tissue-Tec OCT Compound (Sakura Finetek Japan, Tokyo, Japan), and frozen on dry ice and stored at −20 °C. For immunofluorescence staining, 6-μm-thick sections were cut with a Cryostat (Leica Microsystems AG, Wetzlar, Germany). After washing, the sections were treated with 0.1% trypsin (Difco Laboratories, Detroit, MI) in PBS for 30 min at 37 °C to activate antigens. Then the sections were blocked with normal goat serum for 1 h before incubation with polyclonal anti-mouse osteocalcin antibody (1:250, Takara Bio Inc., Shiga, Japan). Subsequently, sections were stained with Alexa Fluor 546 goat anti-rabbit secondary antibody (Molecular Probes, Eugene, OR) for 2 h. Then, sections were stained with 4′,6-diamidino-2-phenylindole (DAPI) for 10 min at room temperature and mounted with anti-fade solution VECTOR Shield (Vector Laboratories, Inc., Burlingame, CA).

GFP and tartrate-resistant acid phosphatase (TRAP) double staining of the ectopic bone. For GFP immunohistochemistry, 6-μm-thick sections of BMP-2-induced ectopic bone were treated with 0.6% hydrogen peroxide in 80% methanol for 30 min and then 3% hydrogen peroxide in PBS for 15 min to inhibit endogenous peroxidase. Then the sections were blocked with normal goat serum for 1 h before incubation with polyclonal anti-GFP antibody (1:250, MBL, Nagoya, Japan). Signals were detected using diaminobenzidine. Subsequently, to detect osteoclasts, TRAP staining was carried out using a staining kit (Cell Garage, Tokyo, Japan) according to the manufacturer's protocol. Counterstaining was performed with hematoxylin.

Culture of MOPCs in PBMNCs. Peripheral blood was taken from the heart of BMP-2-implanted mice with a 24-gauge needle and 1-ml syringe containing heparin and enriched for light-density mononuclear cells (PBMNCs) by Ficoll-Paque (Amersham Biosciences AB, Uppsala, Sweden) centrifugation. Red blood cells were removed by resuspending in 0.125% Tris–NH_4Cl buffer and sieving through a nylon mesh. To culture MOPCs, were then inoculated in basal medium consisting of DMEM supplemented with 10% FCS, 100 U/mL streptomycin/penicillin, and 50% conditioned culture medium (DMEM with 10% FCS) of mouse bone marrow-mesenchymal cells as a growth factor supplement (Otsuru and Tamai, unpublished data). To induce osteoblast differentiation, those cells were cultured in the osteogenic medium consisting of IMDM supplemented with 0.1 μM dexamethasone (Nacalai Tesque, Kyoto, Japan), 10 mM β-glycerol phosphate (Sigma, Saint Louis, MO), and 0.05 mM ascorbic acid 2-phosphate (Sigma) for 3–4 weeks. Cells were then fixed with 4% paraformaldehyde for 10 min and treated with 0.2% Triton X in phosphate-buffered saline (PBS) for 10 min.

Immunostaining of cultured MOPCs. Cultured MOPCs were pretreated with 3% skim milk (Nacalai Tesque) in PBS for 1 h before incubation with polyclonal anti-mouse osteocalcin antibody (1:250, Takara Bio Inc.), monoclonal anti-mouse alkaline phosphatase antibody (1:250, R&D Systems, Minneapolis, MN) or polyclonal anti-mouse osteopontin antibody (1:250, LSL, Tokyo, Japan). Subsequently, sections were stained with Alexa Fluor 546 goat anti-rabbit or anti-rat IgG secondary antibody (Molecular Probes) for 2 h. Those cells were stained with 4′,6-diamidino-2-phenylindole (DAPI) for 10 min at room temperature and mounted with the anti-fade solution VECTOR Shield (Vector Laboratories, Inc.).

Passive transfer of PBMNCs from BMP-2-implanted GFP-mouse to BMP-2-implanted nude mouse. For passive transfer of PBMNCs containing MOPCs, nude mice implanted with BMP-2-containing collagen pellets were injected with PBMNCs from the GFP-transgenic BMP-2-implanted mice via a tail vein. Injections were carried out everyday for one week.

Results

Bone marrow-derived cells contribute to BMP-2-induced ectopic bone formation

We first evaluated whether bone marrow-derived cells are involved in the process of BMP-2-induced ectopic bone formation. We implanted BMP-2 pellets under the muscular fascia in the backs of GFP-BMT mice that had been transplanted with GFP-transgenic bone marrow cells after lethal dose irradiation (Fig. 1A). Three weeks after the implantation of BMP-2 collagen pellets, intense GFP fluorescence had accumulated in the region of the BMP-2-induced ectopic bone (Fig. 1B). Immunohistological analysis revealed that a significant number of GFP-positive cells expressing osteocalcin (OC) were seen lining the newly generated bone (Fig. 1C). Tartrate-resistant acid phosphatase (TRAP) and GFP double staining revealed that some of the GFP-positive lining cells were TRAP-positive osteoclasts, which were clearly distinguishable from GFP-positive/TRAP-negative positive cells (Fig. 1D).

Successful culture of OPCs in PBMNCs from a BMP-2-implanted mouse

To determine if a BMP-2-implanted mouse contained OPCs in circulating blood, we isolated PBMNCs from a BMP-2-implanted mouse and cultured those cells in the con-

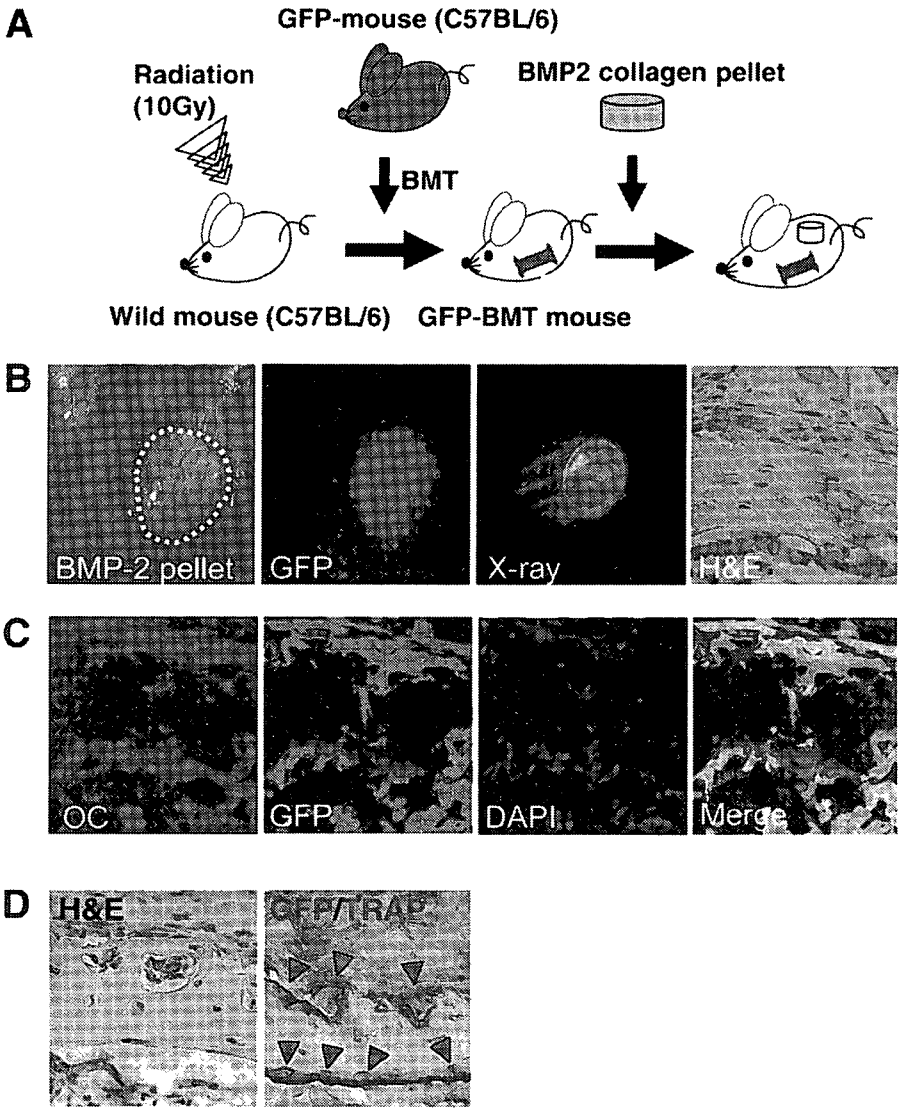

Fig. 1. Bone marrow-derived osteoblast progenitor cells contribute to BMP-2-induced ectopic bone formation in GFP-BMT mice. (A) A BMP-2 pellet is shown implanted under the muscular fascia of a GFP-BMT mouse. (B) A BMP-2 pellet shows accumulation of GFP fluorescence three weeks after implantation. Soft X-ray photo of the BMP-2 pellet demonstrates that ectopic bone has formed in the BMP-2 pellet. Histologic section stained with hematoxylin and eosin (H&E) of the BMP-2 pellet also reveals bone formation in the BMP-2 pellet. Magnification, 400×. (C) Immunofluorescence staining shows that cells lining the newly generated ectopic bone are osteoblasts expressing osteocalcin (OC), and that some of those cells show GFP fluorescence (GFP), revealed as yellow-colored cells in merged picture (Merge) of OC, GFP and DAPI staining (DAPI). Magnification, 400×. (D) GFP and TRAP double staining reveals that the bone marrow-derived osteoclasts (red arrow-head) as well as bone marrow-derived non-osteoclastic cells (brown arrow-head) line the newly formed ectopic bone. Magnification, 400×.

ditioned culture medium, as described in the methods section (Fig. 2A). As we expected, adhesive stromal type cells successfully expanded in culture. Then we looked at the expression of osteoblast-specific proteins before and after induction of osteogenic differentiation. OP, a marker of undifferentiated osteoblasts, was shown to be expressed in the cultures without induction of differentiation (Fig. 2B). Under these culture conditions, however, the differentiation-specific makers ALP and OC were not expressed (Fig. 2B). After change of culture medium to the osteogenic medium, however, these cells then expressed and secreted abundant ALP and OC as well as OP in the culture medium (Fig. 2C).

Intravenous transplantation of GFP-PBMNCs provides GFP-osteoblasts in the ectopic bone in the BMP-2-implanted nude mouse

To confirm further that significant numbers of MOPCs mobilize from bone marrow to peripheral blood and contribute to ectopic bone formation, we isolated PBMNCs

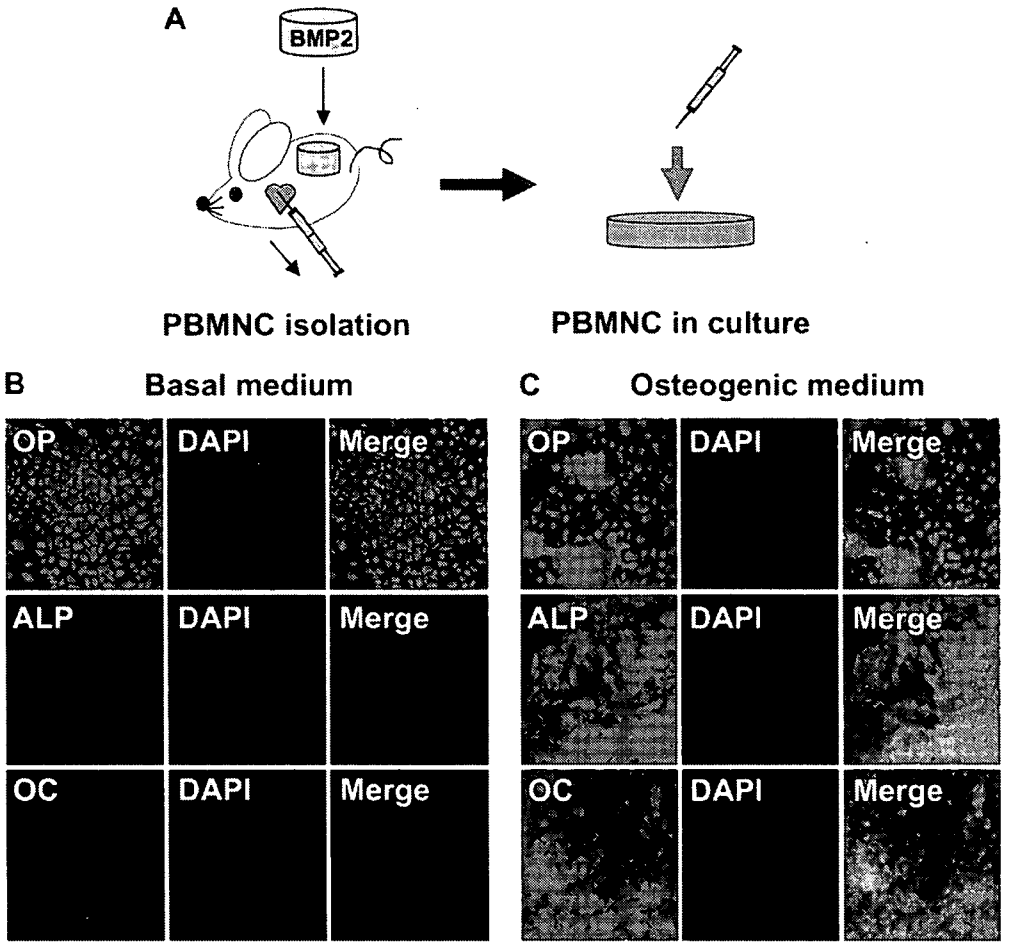

Fig. 2. OPCs in PBMNCs from a BMP-2-implanted mouse express bone matrix proteins in culture. (A) Cultured PBMNCs isolated from peripheral blood of a BMP-2-implanted mouse. (B) Immunofluorescence staining of the cultured cells from isolated PBMNCs shows only osteopontin (OP) expression in normal medium. (C) When those cells were cultured in osteogenic medium, however, there is positive immunoreactivity for alkaline phosphatase (ALP) and osteocalcin (OC) as well as OP. The staining patterns and DAPI staining (DAPI) are shown in the merged image (Merge). Magnification, 200×.

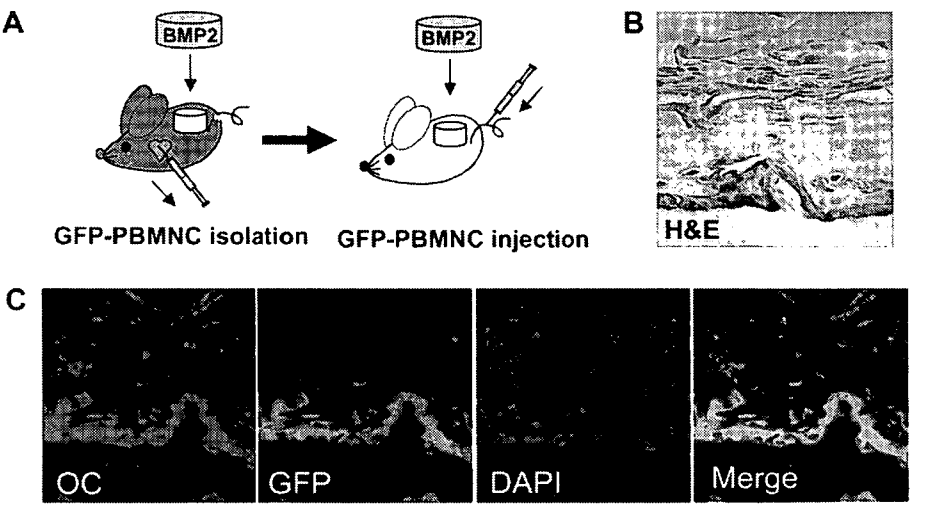

Fig. 3. OPCs in PBMNCs can contribute to ectopic bone formation in a BMP-2 pellet. (A) A nude mouse implanted with a BMP-2 pellet is injected daily for 7 days with PBMNCs taken from BMP-2-implanted GFP transgenic mice. (B) A histologic H&E-stained section shows ectopic bone formation in the BMP-2 pellet. Magnification, 400×. (C) Immunofluorescence staining of the newly generated ectopic bone shows that osteocalcin-expressing osteoblasts (OC) and GFP-positive cells derived from the injected PBMNCs (GFP) co-localize with yellow-colored cells in the merged picture (Merge) with DAPI staining (DAPI). Magnification, 400×.

everyday from BMP-2 pellet-implanted GFP-transgenic mice and injected the isolated PBMNCs (1×10^6) through the tail veins of BMP-2 pellet-implanted nude mice daily for 7 days (Fig. 3A). Two weeks later, the implanted pellets were recovered and examined histologically. We observed that GFP-positive osteoblasts originating from the injected PBMNCs contributed significantly to ectopic bone formation in the mice (Fig. 3B).

Discussion

Circulating mesenchymal precursor/stem cells or osteoblast lineage cells have been shown to exist in various mammals, including humans and mice [4–6,8,9]. Moreover, those circulating mesenchymal/osteoblast lineage cells have been isolated from peripheral blood, expanded in culture, and inoculated to show their potency to become osteoblasts both *in vitro* and *in vivo*. Nevertheless, a number of important questions have been raised following those observations, including as to where those circulating cells came from and where they went *in vivo*? In this study, we have shown, for the first time, clear evidence that marrow cells in intact bone are the major, if not the exclusive, source of circulating OPCs in an *in vivo* model of ectopic bone formation using BMP-2-stimulation in mouse muscle. Of note, our GFP-BMT mouse model showed that ~40% of osteocalcin-producing cells in the ectopic bone were derived from MOPCs, suggesting that endogenous circulating MOPCs may contribute to ectopic bone formation observed in various pathological conditions, and possibly, to fracture healing. Other findings that showed the need for adequate blood flow to obtain mature bone regeneration also add credence to the importance of MOPCs in the circulation [10].

Currently, little is known about the signals that trigger the migration of OPCs from the bone marrow into the circulation and this was not addressed in detail in the current study. Vascular endothelial growth factor (VEGF) previously has been shown to have the capacity to recruit marrow-derived vascular endothelial progenitor cells [11] and we also observed elevation of VEGF levels in the muscle around the implanted BMP-2 pellets (data not shown). This observation may suggest that VEGF contributes to angiogenesis in the area of bone regeneration, although further evidence is needed to support this hypothesis.

The importance of providing additional OPCs to sites of new bone formation has been shown in a number of previous studies [12–17]. From a clinical perspective, identification of signals that induce migration of MOPCs into the circulation could have potential future clinical applications, since increasing MOPCs in the circulation may help patients with delayed or non-union of bone fractures by increasing the number of MOPCs at the bone repair site. The ability to induce circulating MOPCs to enter the peripheral blood circulation may also enable us to easily isolate these cells by simple venous blood sampling, thus providing an opportunity to develop novel cell-based regenerative therapies for bone fractures and possibly for other damaged tissues. Because current procedures to isolate mesenchymal cells directly from the bone marrow are invasive and carry a possible risk of bone marrow infection, the easier approach of isolating MOPCs from peripheral blood has advantages in terms of safety, repeatability, and acceptability. In addition, this method may also be helpful in developing new therapies for genetic disorders such as osteogenesis imperfecta through genetic manipulation of isolated MOPCs [18,19]. Thus, further investigation of circulating MOPCs is warranted to more precisely characterize their cell biology and the mechanisms that lead to their induction. Such work may have very exciting implications for novel therapeutic strategies in bone regenerative medicine.

Acknowledgments

This work was partially supported by Funds of the Ministry of Education, Culture, Sports, Science and Technology, and Grant-in-Aids from the Ministry of Public Health and Welfare. We would like to thank Professor John A McGrath for his technical support.

References

[1] J.M. Wozney, V. Rosen, A.J. Celeste, L.M. Mitsock, M.J. Whitters, R.W. Kriz, R.M. Hewick, E.A. Wang, Novel regulators of bone formation: molecular clones and activities, Science 242 (1988) 1528–1534.

[2] K. Takaoka, H. Nakahara, H. Yoshikawa, K. Masuhara, T. Tsuda, K. Ono, Ectopic bone induction on and in porous hydroxyapatite combined with collagen and bone morphogenetic protein, Clin. Orthop. Relat. Res. (1988) 250–254.

[3] L.C. Gerstenfeld, D.M. Cullinane, G.L. Barnes, D.T. Graves, T.A. Einhorn, Fracture healing as a post-natal developmental process: molecular, spatial, and temporal aspects of its regulation, J. Cell. Biochem. 88 (2003) 873–884.

[4] G.Z. Eghbali-Fatourechi, J. Lamsam, D. Fraser, D. Nagel, B.L. Riggs, S. Khosla, Circulating osteoblast-lineage cells in humans, N. Engl. J. Med. 352 (2005) 1959–1966.

[5] S.A. Kuznetsov, M.H. Mankani, S. Gronthos, K. Satomura, P. Bianco, P.G. Robey, Circulating skeletal stem cells, J. Cell. Biol. 153 (2001) 1133–1140.

[6] C. Wan, Q. He, G. Li, Allogenic peripheral blood derived mesenchymal stem cells (MSCs) enhance bone regeneration in rabbit ulna critical-sized bone defect model, J. Orthop. Res. 24 (2006) 610–618.

[7] M. Okabe, M. Ikawa, K. Kominami, T. Nakanishi, Y. Nishimune, Green mice as a source of ubiquitous green cells, FEBS Lett. 407 (1997) 313–319.

[8] M. Fernandez, V. Simon, G. Herrera, C. Cao, H. Del Favero, J.J. Minguell, Detection of stromal cells in peripheral blood progenitor cell collections from breast cancer patients, Bone Marrow Transplant. 20 (1997) 265–271.

[9] C.A. Roufosse, N.C. Direkze, W.R. Otto, N.A. Wright, Circulating mesenchymal stem cells, Int. J. Biochem. Cell Biol. 36 (2004) 585–597.

[10] J. Glowacki, Angiogenesis in fracture repair, Clin. Orthop. Relat. Res. (1998) S82–S89.

[11] M. Grunewald, I. Avraham, Y. Dor, E. Bachar-Lustig, A. Itin, S. Yung, S. Chimenti, L. Landsman, R. Abramovitch, E. Keshet, VEGF-induced adult neovascularization: recruitment, retention, and role of accessory cells, Cell 124 (2006) 175–189.

[12] L.J. Curylo, B. Johnstone, C.A. Petersilge, J.A. Janicki, J.U. Yoo, Augmentation of spinal arthrodesis with autologous bone marrow in a rabbit posterolateral spine fusion model, Spine 24 (1999) 434–438, discussion 438–439.
[13] R.E. Grundel, M.W. Chapman, T. Yee, D.C. Moore, Autogeneic bone marrow and porous biphasic calcium phosphate ceramic for segmental bone defects in the canine ulna, Clin. Orthop. Relat. Res. (1991) 244–258.
[14] T.S. Lindholm, O.S. Nilsson, T.C. Lindholm, Extraskeletal and intraskeletal new bone formation induced by demineralized bone matrix combined with bone marrow cells, Clin. Orthop. Relat. Res. (1982) 251–255.
[15] T.S. Lindholm, P. Ragni, T.C. Lindholm, Response of bone marrow stroma cells to demineralized cortical bone matrix in experimental spinal fusion in rabbits, Clin. Orthop. Relat. Res. (1988) 296–302.
[16] K. Takagi, M.R. Urist, The role of bone marrow in bone morphogenetic protein-induced repair of femoral massive diaphyseal defects, Clin. Orthop. Relat. Res. (1982) 224–231.
[17] J.R. Werntz, J.M. Lane, A.H. Burstein, R. Justin, R. Klein, E. Tomin, Qualitative and quantitative analysis of orthotopic bone regeneration by marrow, J. Orthop. Res. 14 (1996) 85–93.
[18] J.R. Chamberlain, U. Schwarze, P.R. Wang, R.K. Hirata, K.D. Hankenson, J.M. Pace, R.A. Underwood, K.M. Song, M. Sussman, P.H. Byers, D.W. Russell, Gene targeting in stem cells from individuals with osteogenesis imperfecta, Science 303 (2004) 1198–1201.
[19] E.M. Horwitz, D.J. Prockop, L.A. Fitzpatrick, W.W. Koo, P.L. Gordon, M. Neel, M. Sussman, P. Orchard, J.C. Marx, R.E. Pyeritz, M.K. Brenner, Transplantability and therapeutic effects of bone marrow-derived mesenchymal cells in children with osteogenesis imperfecta, Nat. Med. 5 (1999) 309–313.

ORIGINAL ARTICLE

STAT5a/PPARγ Pathway Regulates Involucrin Expression in Keratinocyte Differentiation

Xiuju Dai[1], Koji Sayama[1], Yuji Shirakata[1], Yasushi Hanakawa[1], Kenshi Yamasaki[1], Sho Tokumaru[1], Lujun Yang[1], Xiaoling Wang[1], Satoshi Hirakawa[1], Mikiko Tohyama[1], Toshimasa Yamauchi[2,3], Kadowaki Takashi[2,3], Hiroyuki Kagechika[4] and Koji Hashimoto[1]

Signal transducers and activators of transcription (STATs) are critical to growth factor-mediated intracellular signal transduction. We observed the rapid expression and activation of STAT5a during keratinocyte differentiation induced by suspension culture. STAT5a expression preceded that of involucrin, an important molecule in the terminal differentiation of keratinocytes. To determine whether STAT5a regulated involucrin expression, we expressed a dominant-negative (dn) STAT5a that blocks the dimerization of STAT5 and inhibits its nuclear translocation. We found that dn-STAT5a inhibited involucrin expression in keratinocytes. Given that STAT5 regulates adipogenesis via activating the peroxisome proliferator-activated receptor (PPAR) γ signal, we hypothesized that STAT5a regulated involucrin expression in the same manner. To test this hypothesis, we examined the expression and transactivation of PPARγ in a suspension culture of keratinocytes. Suspension culture induced PPARγ expression and triggered PPARγ transactivation rapidly and dn-STAT5a downregulated this induction and suppressed PPARγ transactivation. Furthermore, preincubation with the PPARγ/retinoid X-receptor inhibitor HX-531 or the introduction of a dn-PPARγ prevented the activation of involucrin promoter and inhibited its induction. This report provides early evidence of a major role for STAT5a in the differentiation of keratinocytes, where it contributes to involucrin expression by activating the PPARγ signal.

Journal of Investigative Dermatology (2007) **127**, 1728–1735; doi:10.1038/sj.jid.5700758; published online 1 March 2007

INTRODUCTION

Signal transducers and activators of transcription (STATs) are a family of transcription factors that are essential for intracellular signaling in response to stimulation by cytokines, growth factors, and hormones (Horvath, 2000). STAT proteins form homo- or heterodimers on tyrosine phosphorylation and dimerized STAT proteins immediately enter the nucleus, where they bind to specific DNA sequences in the promoters of various genes and mediate transcriptional regulation. In mammals, seven STAT proteins have been identified, including two highly similar STAT5 isoforms. Although STAT5a and STAT5b are roughly 95% similar at the cDNA level, they exhibit both redundant and nonredundant functions *in vivo*, probably because of differences in their transactivation domains (Grimley *et al.*, 1999). STAT5s are involved in a variety of cellular processes, as has been demonstrated in STAT5 knockout mice (Coffer *et al.*, 2000; Levy and Gilliland, 2000). Adipogenesis is a complex process controlled by the interplay of signals emanating from both environmental and intracellular factors. STAT5s are reported to function in fat-cell development, adipocyte differentiation, and lipid accumulation by regulating peroxisome proliferator-activated receptor (PPAR)γ and CCAAT-enhancer binding proteins α signals (Stephens *et al.*, 1999; Nanbu-Wakao *et al.*, 2002; Floyd and Stephens, 2003; Stewart *et al.*, 2004).

PPARs are transcription factors belonging to the ligand-activated nuclear hormone receptor superfamily. Upon binding exogenous or endogenous ligands, PPARs form heterodimers with the retinoid X receptor (RXR), recruit a coactivator, and facilitate the transcription of target genes involved in many cellular functions, including differentiation (Kuenzli and Saurat, 2003). All of the PPAR superfamily members – PPARα, PPARβ/δ, and PPARγ – have been identified in keratinocytes and have been shown to play physiological roles in epidermopoiesis, such as in keratinocyte proliferation and differentiation (Kuenzli and Saurat, 2003).

Although the function of STAT5 has been studied in several cell types, its roles in skin and keratinocytes are unclear, despite the observation of its *in vivo* and *in vitro* expression in human keratinocytes (Poumay *et al.*, 1999; Nishio *et al.*, 2001). We hypothesized that STAT5 is involved in keratinocyte differentiation because it is expressed to a

[1]*Department of Dermatology, Ehime University School of Medicine, Ehime, Japan;* [2]*Department of Integrated Molecular Science on Metabolic Diseases, Graduate School of Medicine, University of Tokyo, Tokyo, Japan;* [3]*Department of Metabolic Diseases, Graduate School of Medicine, University of Tokyo, Tokyo, Japan and* [4]*School of Biomedical Science, Tokyo Medical and Dental University, Tokyo, Japan*

Correspondence: Dr Koji Sayama, Department of Dermatology, Ehime University School of Medicine, Toon, Ehime 791-0295, Japan. E-mail: sayama@m.ehime-u.ac.jp

Abbreviations: Ax, adenovirus vector; m.o.i., multiplicity of infection; PPAR, peroxisome proliferator-activated receptor; RT-PCR, reverse transcriptase-PCR; STATs, signal transducers and activators of transcription

Received 18 July 2006; revised 19 November 2006; accepted 19 December 2006; published online 1 March 2007

substantial degree in the granular layer and in the horny keratinized cells of the epidermis (Nishio *et al.*, 2001). We present evidence that STAT5a is activated and essential for involucrin expression in suspension cultures of keratinocytes. We further demonstrate that STAT5a regulates PPARγ activation, which contributes to involucrin expression during keratinocyte differentiation. This report demonstrates early evidence of a vital role for STAT5a in involucrin expression.

RESULTS

Rapid induction of STAT5a but not STAT5b during keratinocyte differentiation

We investigated the expression of STAT5s in a suspension culture model of keratinocyte differentiation (Watt *et al.*, 1988). For the suspension cultures, we used polyhydroxyethylmethacrylate-coated culture plates, which inhibit cell-to-extracellular matrix interactions but not cell-to-cell interactions (Wakita and Takigawa, 1999). The expression of mRNAs for both STAT5a and STAT5b was detected in the suspension culture. STAT5a mRNA started to increase at 3 hours, reached a peak at 12 hours, and was induced more than 20-fold; the STAT5b mRNA level did not change during suspension culture (Figure 1a). Immunoblotting confirmed the mRNA data: STAT5a protein increased within 6 hours and peaked at 24 hours, whereas the level of STAT5b remained unchanged (Figure 1b). We used a phospho-specific antibody to examine STAT5 phosphorylation at conserved tyrosine, which is required for the activation of STAT5 (Grimley *et al.*, 1999). As shown in Figure 1b, STAT5 was rapidly phosphorylated in cell suspension and the level of phosphorylated STAT5 varied with the level of total STAT5a protein. Next, we investigated the nuclear translocation of STAT5s. After suspension culture, the cells were harvested at the indicated times and the levels of STAT5a, phospho-STAT5, and STAT5b in the nuclear fraction were determined using Western blots. As shown in Figure 1c, STAT5a and phospho-STAT5 were definitely detected in the nucleus beginning at 6 hours in suspension culture, implying that suspension culture triggers the nuclear translocation of phosphorylated STAT5a. In contrast, STAT5b protein was only detected weakly in the nuclear fraction and its level in suspension culture remained constant. These data suggest that STAT5a is transactivated during keratinocyte differentiation induced by suspension culture.

Involucrin expression has been analyzed as an important marker of keratinocyte differentiation (Eckert *et al.*, 2004). In suspension culture, involucrin was induced in a time-dependent manner and occurred after the activation of STAT5a (Figure 1a and b). These data suggested the possibility of a causal relationship between STAT5a and involucrin expression.

Regulation of involucrin expression by STAT5a during keratinocyte differentiation

To explore the function of STAT5a in involucrin expression, we constructed an adenovirus expression vector (Ax) carrying a dominant-negative (dn) mutant of STAT5a (Axdn-STAT5a) that inhibits the dimerization of phosphorylated STAT5a, a

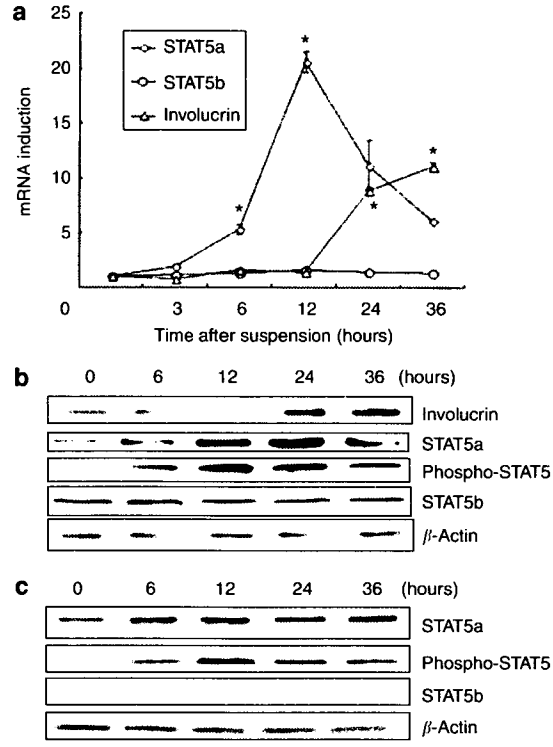

Figure 1. Suspension culture resulted in the induction and activation of STAT5a. (**a**) Keratinocytes were plated onto polyhydroxyethylmethacrylate-coated plates and cultures were incubated for the indicated times. Total RNA was collected and real-time RT-PCR was performed to detect the mRNA levels of STAT5a, STAT5b, and involucrin. The relative mRNA expression levels were expressed as the mean ± SD ($n = 3$). An asterisk indicates significant deviation from the control ($P < 0.05$). (**b**) Suspension cultures were established and cells were collected after the indicated times of incubation. Total protein samples were analyzed by Western blotting with antibodies against involucrin, STAT5a, STAT5b, and phospho-STAT5. The data shown are representative of three separate experiments. (**c**) Keratinocytes were collected at the indicated times after suspension culture. The nuclear fraction was subjected to antibodies against STAT5a, phospho-STAT5, and STAT5b. The data shown are representative of three separate experiments.

key step required for nuclear translocation and DNA binding (Ariyoshi *et al.*, 2000), and infected keratinocytes at different multiplicities of infection (m.o.i.). After 24 hours, sufficient STAT5a protein expression was detected with an m.o.i. of 50 (Figure 2a). To investigate the role of STAT5a in the activation of the involucrin promoter, we performed a luciferase assay. Keratinocytes transfected with an involucrin promoter-luciferase reporter plasmid (pINV-Luc) were infected with adenovirus at an m.o.i. of 50 and then subjected to suspension culture for 24 hours. The reporter activity increased about sevenfold in suspension culture, which was significantly suppressed by dn-STAT5a (Figure 2b). Subsequently, we also examined the influence of dn-STAT5a on involucrin mRNA and protein expression. Infection with Axdn-STAT5a suppressed the suspension culture-induced expression of involucrin mRNA (Figure 2c) and protein (Figure 2d) by more than 50%. These data unequivocally

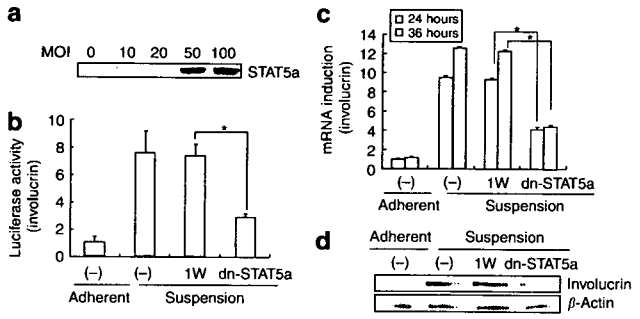

Figure 2. dn-STAT5a-inhibited involucrin expression. (**a**) Subconfluent keratinocytes were infected with Ax carrying dn-STAT5a at different m.o.i. values. After 24 hours, cells were collected and the protein level of STAT5a was detected by immunoblotting. (**b**) Keratinocytes were transfected with involucrin reporter plasmid (pINV-Luc) and pRL-TK (*Renilla* luciferase) using FuGENE6. After 24 hours, the cells were infected with Ax1W or Axdn-STAT5a and cultured for an additional 24 hours. Then, the cells were subjected to suspension culture for 24 hours. Luciferase activity was measured using the Dual-Luciferase reporter assay system. Transfection was performed in triplicate. The relative luciferase activity was calculated by normalizing to the *Renilla* luciferase activity and is presented as the mean ± SD ($n = 3$). An asterisk indicates significant deviation ($P < 0.05$). (**c**) Keratinocytes were infected with Axdn-STAT5a or a control (Ax1W) for 24 hours and suspension cultures were established. Total RNA was collected 24 or 36 hours post-suspension and involucrin mRNA detected by real-time RT-PCR. The involucrin mRNA expression is presented as the mean ± SD ($n = 3$). An asterisk indicates significant deviation ($P < 0.05$). (**d**) Keratinocytes were infected with Axdn-STAT5a or Ax1W for 24 hours before suspension culture. Cells were collected 36 hours after suspension and the level of involucrin protein was evaluated on Western blots. The data shown are representative of three separate experiments.

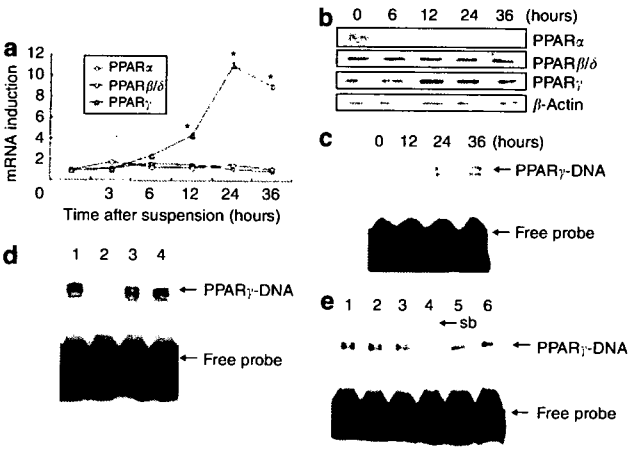

Figure 3. Suspension culture activated PPARγ. (**a**) Total RNA was collected as described in Figure 1a and the mRNA levels of PPAR family members were evaluated by real-time RT-PCR. The relative mRNA expression levels are expressed as the mean ± SD ($n = 3$). An asterisk indicates significant deviation from the control ($P < 0.05$). (**b**) Keratinocytes were subjected to suspension culture for the indicated times. PPARα, β/δ, and γ protein levels were detected by immunoblotting. (**c**) Keratinocytes were subjected to suspension culture and nuclear extracts were collected at the indicated times. Biotin-labeled PPARγ probe was incubated with nuclear protein and EMSA was performed. (**d**) Nuclear extracts from keratinocytes of 24-hour suspension culture were incubated with biotin-labeled PPARγ. Lane 1: no addition of unlabeled probe; lane 2: addition of unlabeled probe for PPARγ; lane 3: addition of unlabeled PPARα probe; lane 4: addition of unlabeled PPARβ/δ probe. (**e**) Nuclear extracts from keratinocytes of 24-hour suspension culture were mixed with biotin-labeled PPARγ probe in the presence of antibodies. Note the supershifted PPARγ-DNA complex seen using an anti-PPARγ antibody (sb: supershifted band). Lane 1: no antibody added; lanes 2–6: addition of normal goat IgG, normal rabbit IgG, goat anti-PPARγ, rabbit anti-PPARα, and rabbit anti-PPARβ/δ, respectively. The data shown are representative of three separate experiments.

defined a positive role of STAT5a in the expression of involucrin during keratinocyte differentiation.

Inducible expression and transactivation of PPARγ during keratinocyte differentiation

Human involucrin promoter activity is complex and cell type-specific. The involucrin promoter contains binding sites for transcription factors of the activator protein-1, Sp-1, and CCAAT-enhancer binding protein families, but no STAT-binding site has been detected (Eckert *et al.*, 2004). Thus, STAT5a must regulate involucrin expression in an indirect manner.

We hypothesized that STAT5a acts on involucrin expression by controlling the PPARγ signal, given that STAT5a/PPARγ functions in adipocyte differentiation (Nanbu-Wakao *et al.*, 2002; Floyd and Stephens, 2003). We first examined the expression of PPARs in suspension cultures of keratinocytes. As shown in Figure 3a and b, PPARα and PPARβ/δ remained relatively constant during culture, whereas the expression of PPARγ mRNA and protein was significantly induced, with expression beginning to increase at 6 hours and peaking at 24 hours after suspension culture. We also performed electrophoretic mobility shift assays (EMSA) to examine the DNA-binding activity of PPARγ in nuclear extracts of keratinocytes. This activity was also induced in suspension culture, and a significant effect was seen between 12 and 36 hours post-suspension (Figure 3c). The PPARγ probe used for EMSA was specific, as the protein–DNA complex was removed by the addition of unlabeled PPARγ probe (lane 2) and was not affected by the presence of the unlabeled probe for PPARα or PPARβ/δ (Figure 3d). The protein–DNA complex could also be supershifted by pre-incubation of nuclear extracts with an antibody specific to PPARγ (lane 4), but not with antibodies to PPARα or β/δ (Figure 3e). Our data suggest that the PPARγ signal was activated in keratinocyte differentiation.

STAT5a regulates the expression and transactivation of PPARγ during keratinocyte differentiation

To investigate whether STAT5a regulates the induction of PPARγ in suspension culture, keratinocytes were infected with Axdn-STAT5a before being subjected to suspension culture and the PPARγ mRNA and protein levels were analyzed. In support of the hypothesis, dn-STAT5a inhibited PPARγ expression in suspension culture (Figure 4a and b), confirming the previous report in adipocytes (Rosen *et al.*, 2000; Nanbu-Wakao *et al.*, 2002; Floyd and Stephens, 2003). In addition, dn-STAT5a almost completely blocked

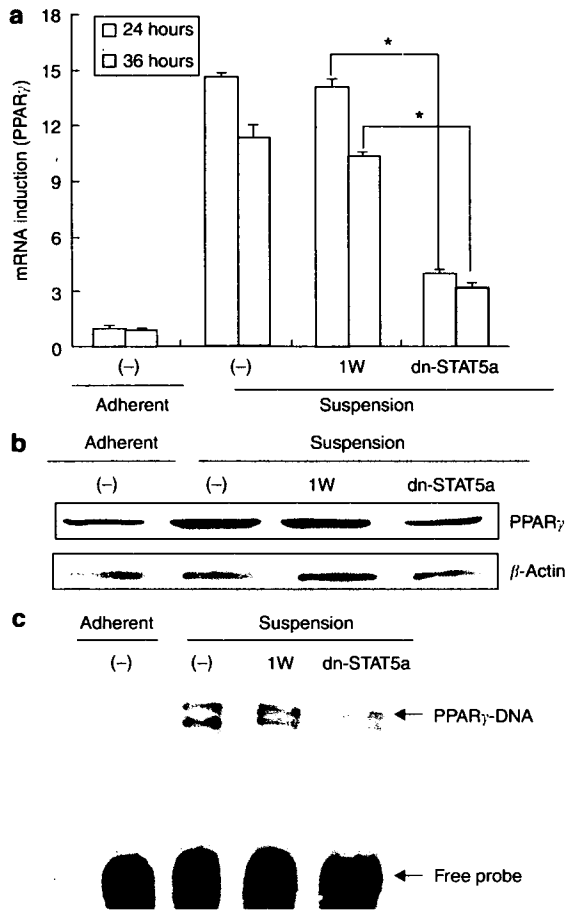

Figure 4. The induction of PPARγ expression by suspension culture was suppressed by dn-STAT5a. RNA samples were prepared as described in Figure 2b. Real-time RT-PCR was performed to detect the level of PPARγ mRNA (**a**) The relative mRNA expression level is expressed as the mean ± SD ($n = 3$). An asterisk indicates significant deviation ($P<0.05$). (**b**) Keratinocytes were infected with Axdn-STAT5a or Ax1W. Cells were collected 24 hours after suspension culture and the level of PPARγ protein was detected on Western blots. (**c**) Keratinocytes were infected with Axdn-STAT5a or Ax1W. Nuclear extracts were collected 24 hour after cell suspension and the DNA-binding activity of PPARγ protein was detected by EMSA. The data shown are representative of three separate experiments.

the DNA-binding activity of PPARγ triggered by suspension culture (Figure 4c). These results indicate that STAT5a regulates the PPARγ signal during keratinocyte differentiation.

Regulation of involucrin expression by PPARγ during keratinocyte differentiation

The treatment of cultured human keratinocytes with ciglitazone, a PPARγ activator, has been shown to increase involucrin and transglutaminase 1 mRNA levels. Moreover, topical treatment of hairless mice with ciglitazone increases both involucrin and filaggrin expression (Mao-Qiang *et al.*, 2004). We found that stimulation with pioglitazone, another PPARγ activator, upregulated involucrin expression in human keratinocytes (data not shown), suggesting that PPARγ activation stimulates the expression of differentiation markers. In this study, we investigated whether PPARγ is important for involucrin expression induced in suspension culture by using HX-531, which has been shown to inhibit significantly PPARγ/RXR transactivation in adipocytes (Yamauchi *et al.*, 2001) and in other epithelial cells (Varley *et al.*, 2004). A luciferase assay was performed to investigate the role of HX531 in activating the involucrin promoter. Keratinocytes transfected with report plasmids were treated with HX531 and then subjected to suspension culture for 24 hours. The suspension culture-increased luciferase activity was inhibited by HX531 (Figure 5a). The expression of involucrin mRNA and protein, which was significantly induced by suspension culture, was also lowered by pretreatment with HX531 (Figures 5b and c). Although it is theoretically possible that HX-531 inhibits vitamin D receptor/RXR activation as an antagonist of RXR, Yamauchi *et al.* (2001) reported that HX-531 had no apparent effect on the transactivation of RXR partners other than PPARγ in adipocytes. In our study, this possibility is unlikely because vitamin D-receptor expression in keratinocytes is anchorage-dependent and is significantly inhibited by suspension culture (Segaert *et al.*, 1998).

We infected keratinocytes with Axdn-PPARγ, which inhibits thiazolidinedione-induced target gene transcription and cellular differentiation in human adipocytes (Gurnell *et al.*, 2000). In human keratinocytes, infection of Axdn-PPARγ at an m.o.i. of 10 resulted in protein expression (Figure 6a) sufficient to inhibit the activation of the involucrin promoter in suspension culture (Figure 6b) and to decrease the involucrin mRNA and protein expression (Figure 6c and d). These data indicate that PPARγ is an important regulator of involucrin transcription and that PPARγ transactivation stimulates involucrin expression during keratinocyte differentiation.

DISCUSSION

The three PPAR isotypes exhibit distinct patterns of tissue distribution. In human epidermis, PPARβ/δ is the prevalent PPAR subtype and PPARα and PPARγ are expressed at lower levels (Kuenzli and Saurat, 2003). In the suspension culture of keratinocytes, the expression and transcriptional activity of PPARγ significantly increased, whereas PPARα expression was unchanged and the PPARβ/δ level remained constantly high. Our data are not completely consistent with the report that in the *ex vivo* differentiation of keratinocytes, the level of PPARβ/δ remained unchanged, whereas PPARα and PPARγ increased significantly (Rivier *et al.*, 1998). In differentiating keratinocytes stimulated by phorbol ester, PPARβ/δ mRNA expression increased (Matsuura *et al.*, 1999) and we have also detected increased expression of PPARβ/δ and PPARγ, but not PPARα, in VD3-induced keratinocyte differentiation (Dai *et al.*, unpublished data). These conflicting data may be attributable to the different differentiation models used. In this study, we demonstrated the important role of PPARγ in involucrin expression by blocking PPARγ/RXR transactivation. The PPARγ ligand has been shown to induce involucrin expression in keratinocytes directly or to act synergistically

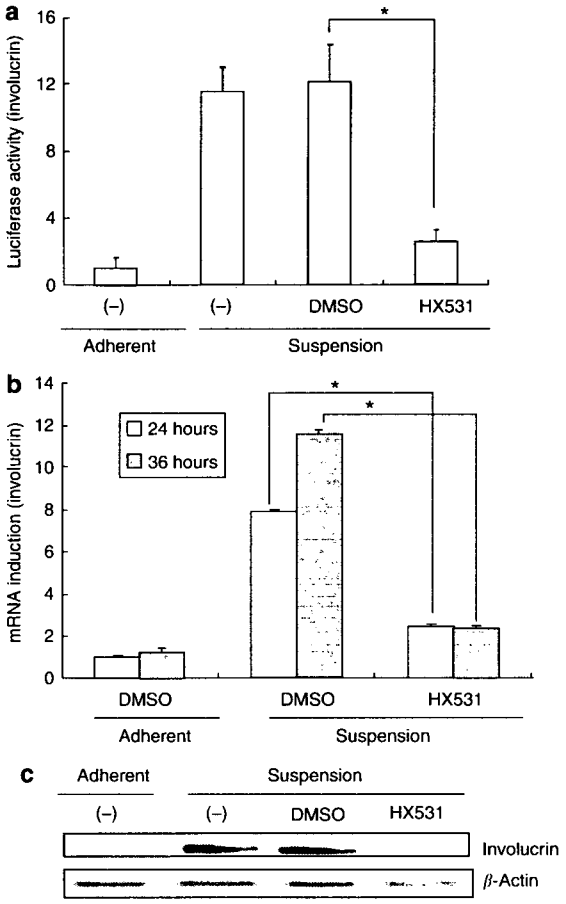

Figure 5. HX-531 suppresses the expression of involucrin. (**a**) The reporter plasmids were introduced into the keratinocytes as described in Figure 2b. After 24 hours, the cells were treated with 1 μM HX-531 or with DMSO for 2 hours and were then subjected to suspension culture for 24 hours. Luciferase activity was measured using the Dual-Luciferase reporter assay system. Transfection was performed in triplicate. The relative luciferase activity was calculated by normalizing to the *Renilla* luciferase activity and is presented as the mean ± SD ($n = 3$). An asterisk indicates significant deviation ($P < 0.05$). (**b**) Keratinocytes were pretreated with 1 μM HX-531 or with DMSO for 2 hours before being subjected to suspension culture. RNA was collected post-suspension and involucrin mRNA was detected by real-time RT-PCR; the relative mRNA expression level is expressed as the mean ± SD ($n = 3$). An asterisk indicates significant deviation ($P < 0.05$). (**c**) Keratinocytes were treated with HX-531 for 2 hours and then subjected to suspension cultures; the cells were collected at 36 hours. The level of involucrin protein was evaluated on Western blot. The data shown are representative of three separate experiments.

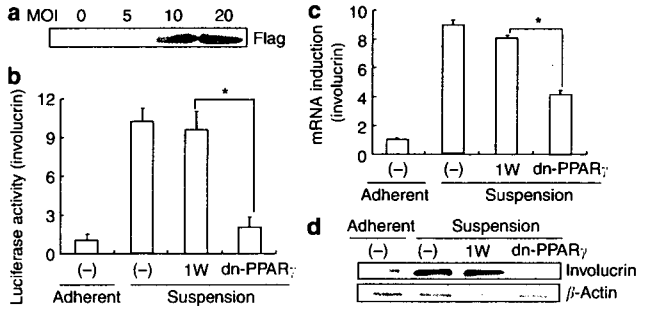

Figure 6. Infection with Axdn-PPARγ inhibited involucrin expression. (**a**) Subconfluent keratinocytes were infected with Axdn-PPARγ at different m.o.i. values. After 24 hours, cells were collected and PPARγ protein was detected by immunoblotting. (**b**) The reporter plasmids (pINV-Luc and pRL-TK) were introduced into the keratinocytes as described in Figure 2b. After 24 hours, the cells were incubated with Ax1W or Axdn-PPARγ for an additional 24 hours. Then, the cells were subjected to suspension culture and the luciferase activity was measured as described in Figure 2b. Transfection was performed in triplicate. The relative luciferase activity was calculated by normalizing to the *Renilla* luciferase activity and is presented as the mean ± SD ($n = 3$). An asterisk indicates significant deviation ($P < 0.05$). (**c**) Keratinocytes were infected with Axdn-PPARγ or Ax1W for 24 hours and suspension cultures were established. Total RNA was collected 30 hours after suspension culture and involucrin mRNA was detected by real-time RT-PCR. The relative mRNA expression level is expressed as the mean ± SD ($n = 3$). An asterisk indicates significant deviation ($P < 0.05$). (**d**) Keratinocytes were infected with Axdn-PPARγ or Ax1W for 24 hours before suspension culture. Cells were collected 36 hours after suspension culture and the level of involucrin protein was evaluated on Western blots. The data shown are representative of three separate experiments.

with other factors (Westergaard *et al.*, 2001; Mao-Qiang *et al.*, 2004). The regulation of differentiation-associated genes by PPARγ has also been reported in other normal epithelia (Varley *et al.*, 2004). The ligands of PPARγ show an ability to regulate cell differentiation and cutaneous homeostasis similar to that of other nuclear hormones, such as glucocorticoids, retinoids, and vitamin D. Treatment with PPARγ-selective ligands has promoted differentiation and normalized the histological features of psoriatic skin in organ culture (Ellis *et al.*, 2000) and in a murine model of epidermal hyperplasia (Demerjian *et al.*, 2006). Together with our study, this suggests that PPARγ probably contributes to keratinocyte differentiation and normalizes epidermal histology by regulating involucrin expression. Although PPARγ functions in involucrin transcription, the PPARγ signal activates the involucrin promoter in a complicated manner and the details are still unclear; it might involve the transcriptional activation of activator protein-1 and CCAAT-enhancer binding proteins (Dai *et al.*, unpublished data).

Our study demonstrated that STAT5a is induced, activated, and involved in involucrin induction, whereas STAT5b expression remains weak and unchanged during suspension culture. Such a difference between isoforms in cell differentiation has been shown previously; STAT5a was sufficient to induce adipogenesis in BALB/C and NIH-3T3 cells, whereas STAT5b alone was not adipogenic. However, the presence of STAT5b enhanced the adipogenic ability of STAT5a (Floyd and Stephens, 2003).

The expression of STAT5 increases early during the course of adipogenesis (Stephens *et al.*, 1999); STAT5 becomes activated during differentiation and it contributes to the enhanced expression of PPARγ (Nanbu-Wakao *et al.*, 2002). Epithelial cell differentiation *in vitro* is reminiscent of adipocyte differentiation in some ways and the ability of STAT5a to induce involucrin expression in suspension culture might be mediated by its ability to regulate PPARγ expression

(Nanbu-Wakao *et al.*, 2002; Floyd and Stephens, 2003). The PPARγ gene produces four different PPARγ mRNAs by alternative splicing and promoter usage. PPARγ1 is expressed ubiquitously (the PPARγ expressed in keratinocytes is mainly PPARγ1), PPARγ2 is restricted to adipose tissue, and PPARγ3 is mainly confined to macrophages, adipose tissue, and the colon (Fajas *et al.*, 1998). The tissue expression of PPARγ4 has not been investigated. Although a putative STAT5-consensus motif in the human PPARγ2 and PPARγ3 promoters has been explored (Nanbu-Wakao *et al.*, 2002; Meirhaeghe *et al.*, 2003), the presence of the STAT5 motif in the PPARγ1 promoter has not been reported (Fajas *et al.*, 1997). Therefore, to elucidate how STAT5a induces PPARγ expression during keratinocyte differentiation and determine whether the PPARγ expressed in skin is a direct target of STAT5a requires further study. Another interesting finding is that blocking the PPARγ signal decreased STAT5a expression in suspension culture slightly (data not shown), implying that the PPARγ and STAT5a signals regulate each other (Olsen and Haldosen, 2006). Although the STAT5a/PPARγ pathway plays a role in involucrin expression, neither STAT5-deficent mice (Coffer *et al.*, 2000; Ikeda *et al.*, 2005) nor PPARγ-deficient mice (Mao-Qiang *et al.*, 2004) show any particular skin defect. This feature can be explained by the fact that blocking the activation of STAT5a or inhibiting the PPARγ signal only partially decreases the inducible expression of involucrin.

Considering all of the available evidence, we suggest that the activation of STAT5a by a challenge to keratinocyte differentiation, such as suspension culture, contributes to involucrin induction by regulating the PPARγ signal. STAT5a thus appears to be an initial transcription factor involved in involucrin expression and keratinocyte differentiation and this study provides early evidence that a STAT5a/PPARγ pathway plays a role in involucrin expression in normal human keratinocytes.

MATERIALS AND METHODS

Keratinocyte culture

Primary normal human keratinocytes were isolated from surgically discarded neonatal skin samples. This study was conducted according to the Declaration of Helsinki Principles and all of the procedures that involved human subjects received prior approval from the Ethics Committee of Ehime University School of Medicine, Japan. All subjects provided written informed consent.

Normal human keratinocytes were cultured in MCDB153 medium supplemented with insulin (1 μg/ml), hydrocortisone (0.5 μg/ml), ethanolamine (0.1 mM), phosphoethanolamine (0.1 mM), bovine hypothalamic extract (50 μg/ml), and Ca^{2+} (0.1 mM), as described elsewhere (Shirakata *et al.*, 2004). Polyhydroxyethylmethacrylate-coated plates were made by coating with a 10-mg/ml solution of polyhydroxyethylmethacrylate (Sigma Chemical, St Louis, MO), and suspension cultures were performed as described previously (Sayama *et al.*, 2002).

Ax construction and Infection

The cosmid cassette pAxCAw and parent virus Ad5-dlX have been described previously (Miyake *et al.*, 1996). The full-length coding region of dn-STAT5a cDNA, a dn mutant with phenylalanine substituted for tyrosine at a phosphorylation site (Ariyoshi *et al.*, 2000; Nanbu-Wakao *et al.*, 2002), was subcloned into pAxCAw. The pcDNA3 expression vector expressing flag-tagged L468A/E471A PPARγ (dn-PPARγ) was a gift from Professor Chatterjee (University of Cambridge, Cambridge, UK). This double-mutant form of PPARγ exhibits impaired transcriptional activity and coactivator recruitment, silences basal transcription by recruitment of corepressors, and is a potent dn inhibitor of wild-type PPARγ activity (Gurnell *et al.*, 2000). The full-length dn-PPARγ cDNA was also cloned into pAxCAw. Adenovirus containing the CA promoter and target gene was generated by the Cosmid-terminal protein complex method (Miyake *et al.*, 1996). Recombinant viruses were generated through homologous recombination in 293 cells; purified virus stocks were prepared by the CsCl gradient method, and the virus titer was checked with a plaque formation assay (Miyake *et al.*, 1996). Cultured normal human keratinocytes were infected with Ax; Ax1W was used as the control vector to exclude the effect of Ax itself, as described previously (Dai *et al.*, 2004).

Real-time RT-PCR

Total RNA samples from cultured cells were isolated using Isogen (Nippon Gene, Tokyo, Japan). Real-time reverse transcriptase-PCR (RT-PCR) was performed and analyzed in an ABI PRISM 7700 sequence detector (PE Applied Biosystems, Branchburg, NJ). The primers and probes for glyceraldehyde-3-phosphate dehydrogenase, STAT5a, STAT5b, involucrin, and PPARs used for real-time PCR were obtained from Applied Biosystems (Norwalk, CT). The RNA analysis was carried out using a TaqMan RT-PCR Master Mix reagents kit (Applied Biosystems). The cDNA synthesis and PCR were performed as described previously (Dai *et al.*, 2004), according to the manufacturers' protocols. The quantification of gene expression was performed using the comparative CT method as described previously (Dai *et al.*, 2004). The target gene expression in the test samples was normalized to the corresponding glyceraldehyde-3-phosphate dehydrogenase gene expression and was reported as the fold difference relative to glyceraldehyde-3-phosphate dehydrogenase.

Western blotting

Keratinocytes were harvested at the indicated times after suspension culture and whole-cell lysates and the nuclear fraction were extracted as described previously (Yahata *et al.*, 2003). Analyses were performed using a Vistra ECF kit (Amersham Biosciences, Arlington Heights, IL) according to the manufacturer's instructions. Twenty micrograms of protein was separated by 10% SDS-PAGE and transferred to nitrocellulose membranes. The membranes were blocked with 5% non-fat dry milk in Tris-HCl (pH 7.4), 0.15 M NaCl, and 0.05% Tween-20, followed by overnight incubation with mouse antibody against STAT5a or STAT5b (ZYMED Laboratories, San Francisco, CA), rabbit anti-phospho-STAT5 (Cell Signaling Technology, Beverly, MA), rabbit anti-involucrin (Biomedical Technologies, Stoughton, MA), mouse anti-PPARγ, goat anti-β-actin (Santa Cruz Biotechnology, Santa Cruz, CA), or rabbit anti-PPARα or β/δ (Abcam, Cambridge, UK). After washing, the membrane was incubated with a 1:2500 dilution of fluorescein-labeled IgG for 1 hour. The signal was amplified with an anti-fluorescein antibody conjugated with alkaline phosphatase, followed by the fluorescent substrate AttoPhos (Amersham Biosciences). The membrane was

then scanned using a FluorolImager (Molecular Dynamics, Sunnyvale, CA).

Preparation of nuclear extracts and EMSA

Nuclear proteins were isolated as described previously (Dignam *et al.*, 1983). Briefly, cells were scraped into a lysis buffer (50 mM 4-(2-hydroxyethyl)-1-piperazineethanesulfonic acid (pH 7.8), 10 mM KCl, 0.1 mM EDTA, pH 8.0, 1 mM dithiothreitol) containing a protease-inhibitor cocktail and 0.5% NP-40. Nuclei were collected by centrifugation and resuspended in 100 μl of 4-(2-hydroxyethyl)-1-piperazineethanesulfonic acid buffer without NP-40 and containing 420 mM KCl and 5 mM $MgCl_2$. After a 30-minute incubation on ice, nuclear debris was removed by centrifugation at 20,000 $\times g$ for 15 minutes at 4°C. Supernatants were collected and stored at −80°C until use.

EMSA was performed using a Light Shift® Chemiluminescent EMSA kit (Pierce, Rockford, IL) according to the manufacturer's instructions. Specific PPARγ, α, and β/δ oligonucleotide probe sets (biotin-labeled and unlabeled probes; Panomics, Redwood City, CA) were used as described (Juge-Aubry *et al.*, 1997). In brief, binding reactions (20 μl) containing 1 × binding buffer, 50 ng/μl poly(dIdC), biotin-labeled PPARγ probe, and nuclear protein (5 μg) were prepared and incubated at room temperature for 20 minutes. In competition experiments, unlabeled probes were added at 100-fold molar excess. For supershift assays, nuclear extracts were preincubated with goat polyclonal anti-PPARγ (Santa Cruz Biotechnology), rabbit polyclonal anti-PPARα or β/δ (Abcam), or with species-matched control IgG for 1 hour at 4°C, followed by the addition of a biotin-labeled PPARγ probe.

Protein–DNA complexes were separated by electrophoresis in 5% native polyacrylamide gels and transferred to Biodyne® B nylon membranes (Pierce). The labeled DNA was cross-linked to the membrane by exposure to 302-nm UV radiation on a UV transilluminator for 1 minute. The biotin-labeled molecules in the membrane were detected using a chemiluminescent nucleic acid detection module (Pierce). The membrane was briefly soaked in a blocking solution, incubated in conjugate/blocking solution for 15 minutes, washed four times in wash buffer and once in substrate equilibration buffer, incubated in substrate working solution for 5 minutes, and exposed to X-ray film.

Luciferase assay

A reporter plasmid containing the involucrin promoter and firefly luciferase (pINV-Luc) was constructed, as described previously (Sayama *et al.*, 2001). To normalize the transfection efficiency, a plasmid containing *Renilla* luciferase driven by the herpes simplex virus thymidine kinase promoter (pRL-TK; Promega, Madison, WI) was included in the assay. The reporter plasmids were introduced into the keratinocytes using FuGENE6 (Roche Molecular Biochemicals, Indianapolis, IN) according to the manufacturer's instructions. After 24 hours, the cells were infected with the indicated adenovirus or treated with HX531 and subjected to suspension culture for 24 hours. Then, the same number of cells was harvested with 250 μl of lysis buffer (Promega) and the luciferase activity was measured using the Dual-Luciferase reporter assay system (Promega) with a luminometer (Luminescencer JNR AB-2100; Atto, Osaka, Japan). The relative luciferase activity was calculated by normalizing to the *Renilla* luciferase activity.

Chemical

HX531 was synthesized as described elsewhere (Yamauchi *et al.*, 2001) and dissolved in DMSO.

Statistical analysis

At least three independent experiments were performed with similar results. One representative experiment is shown in each figure. Statistical significance was determined using Student's paired *t*-test. Differences were considered statistically significant at $P<0.05$ (*).

CONFLICT OF INTEREST

The authors state no conflict of interest.

ACKNOWLEDGMENTS

We thank Teruko Tsuda and Eriko Tan for their excellent technical assistance. This work was supported by grants from the Ministries of Health, Labor, and Welfare and Education, Culture, Sports, Science, and Technology of Japan.

REFERENCES

Ariyoshi K, Nosaka T, Yamada K, Onishi M, Oka Y, Miyajima A *et al.* (2000) Constitutive activation of STAT5 by a point mutation in the SH2 domain. *J Biol Chem* 275:24407–13

Coffer PJ, Koenderman L, de Groot RP (2000) The role of STATs in myeloid differentiation and leukemia. *Oncogene* 19:2511–22

Dai X, Yamasaki K, Shirakata Y, Sayama K, Hashimoto K (2004) All-trans-retinoic acid induces interleukin-8 via the nuclear factor-kappaB and p38 mitogen-activated protein kinase pathways in normal human keratinocytes. *J Invest Dermatol* 123:1078–85

Demerjian M, Man MQ, Choi EH, Brown BE, Crumrine D, Chang S *et al.* (2006) Topical treatment with thiazolidinediones, activators of peroxisome proliferator-activated receptor-gamma, normalizes epidermal homeostasis in a murine hyperproliferative disease model. *Exp Dermatol* 15:154–60

Dignam JD, Martin PL, Shastry BS, Roeder RG (1983) Eukaryotic gene transcription with purified components. *Methods Enzymol* 101:582–98

Eckert RL, Crish JF, Efimova T, Dashti SR, Deucher A, Bone F *et al.* (2004) Regulation of involucrin gene expression. *J Invest Dermatol* 123:13–22

Ellis CN, Varani J, Fisher GJ, Zeigler ME, Pershadsingh HA, Benson SC *et al.* (2000) Troglitazone improves psoriasis and normalizes models of proliferative skin disease: ligands for peroxisome proliferator-activated receptor-gamma inhibit keratinocyte proliferation. *Arch Dermatol* 136:609–16

Fajas L, Auboeuf D, Raspe E, Schoonjans K, Lefebvre AM, Saladin R *et al.* (1997) The organization, promoter analysis, and expression of the human PPARγ gene. *J Biol Chem* 272:18779–89

Fajas L, Fruchart JC, Auwerx J (1998) PPARgamma3 mRNA: a distinct PPARγ mRNA subtype transcribed from an independent promoter. *FEBS Lett* 438:55–60

Floyd ZE, Stephens JM (2003) STAT5A promotes adipogenesis in nonprecursor cells and associates with the glucocorticoid receptor during adipocyte differentiation. *Diabetes* 52:308–14

Grimley PM, Dong F, Rui H (1999) Stat5a and Stat5b: fraternal twins of signal transduction and transcriptional activation. *Cytokine Growth Factor Rev* 10:131–57

Gurnell M, Wentworth JM, Agostini M, Adams M, Collingwood TN, Provenzano C *et al.* (2000) A dominant-negative peroxisome proliferator-activated receptor gamma (PPARgamma) mutant is a constitutive repressor and inhibits PPARgamma-mediated adipogenesis. *J Biol Chem* 275:5754–9

Horvath CM (2000) STAT proteins and transcriptional responses to extracellular signals. *Trends Biochem Sci* 25:496–502

Ikeda K, Nakajima H, Suzuki K, Watanabe N, Kagami S, Iwamoto I (2005) Stat5a is essential for the proliferation and survival of murine mast cells. *Int Arch Allergy Immunol* 137(Suppl 1):45–50

Juge-Aubry C, Pernin A, Favez T, Burger AG, Wahli W, Meier CA *et al.* (1997) DNA binding properties of peroxisome proliferator-activated receptor subtypes on various natural peroxisome proliferator response elements. Importance of the 5'-flanking region. *J Biol Chem* 272: 25252–9

Kuenzli S, Saurat JH (2003) Peroxisome proliferator-activated receptors in cutaneous biology. *Br J Dermatol* 149:229–36

Levy DE, Gilliland DG (2000) Divergent roles of STAT1 and STAT5 in malignancy as revealed by gene disruptions in mice. *Oncogene* 19:2505–10

Mao-Qiang M, Fowler AJ, Schmuth M, Lau P, Chang S, Brown BE *et al.* (2004) Peroxisome-proliferator-activated receptor (PPAR)-gamma activation stimulates keratinocyte differentiation. *J Invest Dermatol* 123: 305–12

Matsuura H, Adachi H, Smart RC, Xu X, Arata J, Jetten AM (1999) Correlation between expression of peroxisome proliferator-activated receptor beta and squamous differentiation in epidermal and tracheobronchial epithelial cells. *Mol Cell Endocrinol* 147:85–92

Meirhaeghe A, Fajas L, Gouilleux F, Cottel D, Helbecque N, Auwerx J *et al.* (2003) A functional polymorphism in a STAT5B site of the human PPAR gamma 3 gene promoter affects height and lipid metabolism in a French population. *Arterioscler Thromb Vasc Biol* 23:289–94

Miyake S, Makimura M, Kanegae Y, Harada S, Sato Y, Takamori K *et al.* (1996) Efficient generation of recombinant adenoviruses using adenovirus DNA-terminal protein complex and a cosmid bearing the full-length virus genome. *Proc Natl Acad Sci USA* 93:1320–4

Nanbu-Wakao R, Morikawa Y, Matsumura I, Masuho Y, Muramatsu MA, Senba E *et al.* (2002) Stimulation of 3T3-L1 adipogenesis by signal transducer and activator of transcription 5. *Mol Endocrinol* 16:1565–76

Nishio H, Matsui K, Tsuji H, Tamura A, Suzuki K (2001) Immunolocalisation of the janus kinases (JAK) – signal transducers and activators of transcription (STAT) pathway in human epidermis. *J Anat* 198:581–9

Olsen H, Haldosen LA (2006) Peroxisome proliferator-activated receptor gamma regulates expression of signal transducer and activator of transcription 5A. *Exp Cell Res* 312:1371–80

Poumay Y, Jolivet G, Pittelkow MR, Herphelin F, De Potter IY, Mitev V *et al.* (1999) Human epidermal keratinocytes upregulate expression of the prolactin receptor after the onset of terminal differentiation, but do not respond to prolactin. *Arch Biochem Biophys* 364:247–53

Rivier M, Safonova I, Lebrun P, Griffiths CE, Ailhaud G, Michel S (1998) Differential expression of peroxisome proliferator-activated receptor subtypes during the differentiation of human keratinocytes. *J Invest Dermatol* 111:1116–21

Rosen ED, Walkey CJ, Puigserver P, Spiegelman BM (2000) Transcriptional regulation of adipogenesis. *Genes Dev* 14:1293–307

Sayama K, Hanakawa Y, Shirakata Y, Yamasaki K, Sawada Y, Sun L *et al.* (2001) Apoptosis signal-regulating kinase 1 (ASK1) is an intracellular inducer of keratinocyte differentiation. *J Biol Chem* 276:999–1004

Sayama K, Yamasaki K, Hanakawa Y, Shirakata Y, Tokumaru S, Ijuin T *et al.* (2002) Phosphatidylinositol 3-kinase is a key regulator of early phase differentiation in keratinocytes. *J Biol Chem* 277:40390–6

Segaert S, Garmyn M, Degreef H, Bouillon R (1998) Anchorage-dependent expression of the vitamin D receptor in normal human keratinocytes. *J Invest Dermatol* 111:551–8

Shirakata Y, Ueno H, Hanakawa Y, Kameda K, Yamasaki K, Tokumaru S *et al.* (2004) TGF-beta is not involved in early phase growth inhibition of keratinocytes by 1alpha,25(OH)2vitamin D3. *J Dermatol Sci* 36:41–50

Stephens JM, Morrison RF, Wu Z, Farmer SR (1999) PPARgamma ligand-dependent induction of STAT1, STAT5A, and STAT5B during adipogenesis. *Biochem Biophys Res Commun* 262:216–22

Stewart WC, Baugh JE Jr, Floyd ZE, Stephens JM (2004) STAT 5 activators can replace the requirement of FBS in the adipogenesis of 3T3-L1 cells. *Biochem Biophys Res Commun* 324:355–9

Varley CL, Stahlschmidt J, Smith B, Stower M, Southgate J (2004) Activation of peroxisome proliferator-activated receptor-gamma reverses squamous metaplasia and induces transitional differentiation in normal human urothelial cells. *Am J Pathol* 164:1789–98

Wakita H, Takigawa M (1999) Activation of epidermal growth factor receptor promotes late terminal differentiation of cell-matrix interaction-disrupted keratinocytes. *J Biol Chem* 274:37285–91

Watt FM, Jordan PW, O'Neill CH (1988) Cell shape controls terminal differentiation of human epidermal keratinocytes. *Proc Natl Acad Sci USA* 85:5576–80

Westergaard M, Henningsen J, Svendsen ML, Johansen C, Jensen UB, Schroder HD *et al.* (2001) Modulation of keratinocyte gene expression and differentiation by PPAR-selective ligands and tetradecylthioacetic acid. *J Invest Dermatol* 116:702–12

Yahata Y, Shirakata Y, Tokumaru S, Yamasaki K, Sayama K, Hanakawa Y *et al.* (2003) Nuclear translocation of phosphorylated STAT3 is essential for vascular endothelial growth factor-induced human dermal microvascular endothelial cell migration and tube formation. *J Biol Chem* 278:40026–31

Yamauchi T, Waki H, Kamon J, Murakami K, Motojima K, Komeda K *et al.* (2001) Inhibition of RXR and PPARgamma ameliorates diet-induced obesity and type 2 diabetes. *J Clin Invest* 108:1001–13

Journal of

An Intermediary Role of proHB-EGF Shedding in Growth Factor-induced *c-Myc* Gene Expression

DAISUKE NANBA,[1] HIROFUMI INOUE,[1] YUKA SHIGEMI,[1] YUJI SHIRAKATA,[2] KOJI HASHIMOTO,[2] AND SHIGEKI HIGASHIYAMA[1,3]*

[1]*Department of Biochemistry and Molecular Genetics, Ehime University Graduate School of Medicine, Shitsukawa, Toon, Ehime, Japan*

[2]*Department of Dermatology, Ehime University Graduate School of Medicine, Shitsukawa, Toon, Ehime, Japan*

[3]*PRESTO, JST, Japan*

Activation of growth factor receptors by ligand binding leads to an increased expression of *c-Myc*, a transcriptional regulator for cell proliferation. The activation of transcriptional factors via the activated receptors is thought to be the main role of *c-Myc* gene expression. We demonstrate here that epidermal growth factor receptor (EGFR)- and fibroblast growth factor receptor (FGFR)-mediated *c-Myc* induction and cell cycle progression in primary cultured mouse embryonic fibroblasts (MEFs) are abrogated by knockout of the *heparin-binding EGF-like growth factor* (*Hb-egf*) gene, or by a metalloproteinase inhibitor, although molecules downstream of the receptors are activated. Induction of *c-Myc* expression by EGF or basic FGF is recovered in *Hb-egf*-depleted MEFs by overexpression of wild-type proHB-EGF, but no recovery was observed with an uncleavable mutant of proHB-EGF. The uncleavable mutant also inhibited EGF-induced acetylation of histone H3 at the mouse *c-Myc* first intron region, which could negatively affect transcriptional activation. We conclude that signal transduction initiated by generation of the carboxyl-terminal fragment of proHB-EGF (HB-EGF-CTF) in the shedding event plays an important intermediary role between growth factor receptor activation and *c-Myc* gene induction.

J. Cell. Physiol. 214: 465–473, 2008.

Growth factors stimulate quiescent cells into DNA synthesis. The transcription factor encoded by the *c-Myc* gene is expressed in a strictly growth factor-dependent manner in quiescent cells (Obaya et al., 1999) and directs gene transcription associated with the transition from quiescence to proliferation. For example, *c-Myc* induces a number of target molecules involved in G1 phase entry into the cell cycle, including Cdc25A, cyclin D2, CDK4, Cul1, and E2F2 (Galaktionov et al., 1996; Leone et al., 1997; Bouchard et al., 1999; Hermeking et al., 2000), supporting the conclusion that *c-Myc* plays a central role in cell cycle progression as an upstream regulator of cell cycle regulatory molecules. Indeed, *c-Myc* null cells are able to survive, but display a marked lengthening of both the G1 and G2 phases of the cell cycle. Although the duration of S phase in *c-Myc* null cells remains unchanged, the G0 to S phase transition is also significantly delayed (Mateyak et al., 1997).

A key step for signaling through the epidermal growth factor receptor (EGFR) is the release of mature ligands such as heparin-binding EGF-like growth factor (HB-EGF) from their membrane-anchored precursor forms, a process referred to as "ectodomain shedding" (Blobel, 2005; Higashiyama and Nanba, 2005). The HB-EGF precursor (proHB-EGF) is cleaved by members of the "a disintegrin and metalloprotease" (ADAM) protease family (Asakura et al., 2002; Blobel, 2005; Higashiyama and Nanba, 2005), yielding the carboxyl terminal fragment of proHB-EGF (HB-EGF-CTF) in parallel with the production of HB-EGF. We have previously characterized HB-EGF-CTF as a novel intracellular signaling molecule that is acquired post-translationally and translocated into the nucleus, where it binds to and inactivates the promyelocytic leukemia zinc finger protein (PLZF) (Nanba et al., 2003). PLZF is a transcriptional repressor that suppresses transcription of genes such as *c-Myc*, *cyclin A2*, and *HoxD11* (Yeyati et al., 1999; Barna et al., 2000; McConnell et al., 2003). Thus, shedding of proHB-EGF participates in activation of two independent signal transduction pathways: signaling from EGFR after engagement of the shed growth factor, and a HB-EGF-CTF-mediated signaling (Higashiyama and Nanba, 2005). Here, we demonstrate that HB-EGF-CTF signaling is involved in growth factor-induced *c-Myc* expression.

Materials and Methods

Materials

12-o-tetradecanoylphorbol-13-acetate (TPA) was purchased from WAKO Pure Chem. Ind., Ltd. (Osaka, Japan). KB-R7785 (Asakura

Contract grant sponsor: Osaka Cancer Research Foundation.
Contract grant sponsor: Ehime University Research Foundation.
Contract grant sponsor: Ministry of Education, Culture, Sports, Science, and Technology of Japan;
Contract grant number: 17014068.
Contract grant sponsor: Precursory Research for Embryonic Science and Technology (Information and Cell Function);
Contract grant number: 17390081.

Daisuke Nanba's present address is Laboratory of Stem Cell Dynamics, School of Life Science, Swiss Federal Institute of Technology, Laussane, Switzerland.

*Correspondence to: Shigeki Higashiyama, Department of Biochemistry and Molecular Genetics, Ehime University Graduate School of Medicine, Shitsukawa, Toon, Ehime 791-0295, Japan.
E-mail: shigeki@m.ehime-u.ac.jp

Received 12 January 2007; Accepted 26 June 2007

DOI: 10.1002/jcp.21233

et al., 2002) and EGFR-neutralizing antibodies were obtained from Carna Biosciences, Inc. (Kobe, Japan) and Immuno-Biological Laboratories Co., Ltd. (Takasaki, Japan), respectively. Recombinant EGF and basic fibroblast growth factor (bFGF) were purchased from R&D Systems, Inc. (Minneapolis, MN).

Cell culture

The fibrosarcoma cell line HT1080 was cultured in Eagle minimum essential medium (EMEM) (Nikken Bio Medical Laboratory, Kyoto, Japan) with 10% fetal calf serum (FCS), 100 units of penicillin G potassium, and 100 μg of streptomycin sulfate per milliliter. The culture of primary human epidermal keratinocytes was prepared as described previously (Hashimoto et al., 1994). E13.5 embryos from loxHB-EGF mice were used to generate mouse embryonic fibroblasts (MEFs). MEFs were maintained in Dulbecco's modified Eagle medium (DMEM) (Nikken) supplemented with 10% FCS, 100 units of penicillin G potassium, and 100 μg of streptomycin sulfate per milliliter. Quiescent MEFs were prepared by serum starvation for 3 days. All cells were cultured in a humidified 37 C/ 5% CO_2 incubator.

Ribonuclease protection assay (RPA)

Total RNA was isolated from keratinocytes (1.0×10^6 cells) or MEFs (2.0×10^6 cells) with Trizol reagent (Invitrogen, Carlsbad, CA). Riboprobes were labeled with digoxigenin (DIG) using the DIG RNA labeling kit (Roche Diagnostics, Basel, Switzerland) according to the manufacturer's protocol. Thirty micrograms of total RNA harvested from cells cultured under each condition were hybridized with DIG-labeled probes. RNase treatment and gel resolution of protected probes were performed according to the manufacturer's protocol with the RPAIII kit (Ambion, Austin, TX). Each value (*c-Myc*/*Gapdh*) was normalized using the value for non-treated cells as taken to be one in each experiment. The values (means ± SD) were determined based on results in at least three independent experiments. *P*-values were obtained from Student's *t*-test.

Immunoprecipitation and immunoblotting

Immunoprecipitation and immunoblotting of cell lysates was performed as described previously (Goishi et al., 1995; Nanba et al., 2003). The primary antibodies used were as follows: mouse monoclonal antibodies to phospho-EGFR (Upstate, Billerica, MA); rabbit polyclonal antibodies to EGFR (Santa Cruz Biotechnology, Santa Cruz, CA), Erk1/2, phospho-Erk1/2 (Cell Signaling Technology, Lexington, KY), anti-β-actin (SIGMA, St. Louis, MO) and anti-HB-EGF-CTF antibodies (H1). Incubations of 1 h were performed with two secondary antibodies: HRP-conjugated goat anti-mouse and rabbit IgG (Promega, Madison, WI).

ProHB-EGF-AP shedding assay

HT1080 cells stably expressing alkaline phosphatase (AP)-tagged proHB-EGF (Asakura et al., 2002) were seeded in 24-well plates at a density of 1.0×10^5 cells per well and incubated for 24 h. Recombinant EGF (final 1–50 ng/ml), and bFGF (final 1–50 ng/ml) were added and the plates were incubated for a further 1 h. pAP-HB-EGF plasmids were transiently transfected into MEFs using a MEF Nucleofector kit (Amaxa Biosystems, Gaithersburg, MD). Twenty-four hours after transfection, the cells were treated with KB-R7785 (final 10–20 μM) and TPA (final 100 nM). Aliquots (100 μl each) of the conditioned media were used to measure AP activity as described previously (Tokumaru et al., 2000).

Immunofluorescence microscopy and visualization of the fluorescent signal intensity

Immunofluorescence microscopy of human keratinocytes using a rabbit polyclonal antibody to HB-EGF-CTF (Miyagawa et al., 1995) was performed as described previously (Nanba et al., 2003). We visualized the intensity of the fluorescent signal in each picture using Scion image (Scion Corporation, Frederick, MD).

Adenovirus construction and infection

Adenovirus vectors carrying genes encoding LacZ, green fluorescent protein (GFP), AP-tagged or non-tagged proHB-EGF, and uncleavable proHB-EGF were prepared using an adenovirus expression kit (Takara Biomedicals, Otsu Japan). An adenovirus expressing Cre recombinase (Kanegae et al., 1995) under the control of the CAG promoter (Niwa et al., 1991) was obtained from RIKEN BRC (Tsukuba, Japan). Purified, concentrated, and titer-checked viruses were applied to cells at a multiplicity of infection (MOI) of 100.

PCR, RT-PCR, and quantitative PCR analysis

Deletion of the mouse *Hb-egf* gene, mRNA expression of EGFR ligands, and *Plzf* in MEFs were confirmed by PCR and RT-PCR analysis, respectively. Primers are shown in Table 1. Quantitative PCR was performed using the ABI Prism 7700 sequencer detection system (Applied Biosystems, Foster, CA) with TaqMan Gene Expression Assay kits (Applied Biosystems) for mouse *c-Myc*

TABLE 1. Primer sequences for PCR and RT-PCR analysis

Primer	Sequence
loxHB-EGF (forward)	5′-CGGACAGTGCCTTAGTGGAACCTC-3′
loxHB-EGF (reverse)	5′-GCTTCTTCTTAGGAGGGAATCTTGGC-3′
Mouse *Hb-egf* (forward)	5′-TGCCGTCGGTGATGCTGAACT-3′
Mouse *Hb-egf* (reverse)	5′-GGTTCAGATCTGTCCCTTCCAAGTC-3′
Mouse *Tgf-α* (forward)	5′-GGAATTCCTAGCGCTGGGTATCCTGTTA-3′
Mouse *Tgf-α* (reverse)	5′-CAAGCTTACCACCACCAGGGCAGTGATG-3′
Mouse *Amphiregulin* (forward)	5′-GCAATTGTCATCAAGATTACTTTGG-3′
Mouse *Amphiregulin* (reverse)	5′-TCTGTTTCTCCTTCATATTCCCTG-3′
Mouse *Epiregulin* (forward)	5′-GGAATTCTGACGCTGCTTTGTCTAGGTT-3′
Mouse *Epiregulin* (reverse)	5′-CAAGCTTTATGCATCCAGCGGTTATGAT-3′
Mouse *Plzf* (forward)	5′-TCAAGAGCCACAAGCGCATCCACA-3′
Mouse *Plzf* (reverse)	5′-CGAGGCACCGTTGTGTGTTCTCA-3′
Mouse *GAPDH* (forward)	5′-CGTATTGGGCGCCTGGTCACCAG-3′
Mouse *GAPDH* (reverse)	5′-TCGCTCCTGGAAGATGGTGATGGG-3′
Region I (forward)	5′-GTGCAATGAGCTCGATGAAGGAAG-3′
Region I (reverse)	5′-GTCTTCTTATTCCGGACTCCTCG-3′
Region II (forward)	5′-TTACTGGACTGCGCAGGGAG-3′
Region II (reverse)	5′-CCACGTATACTTGGAGAGCCACTT-3′
Region III (forward)	5′-GGTAAGCACAGATCTGGTGGTCTT-3′
Region III (reverse)	5′-AAGTCAGAAGCTACGGAGCCTTCT-3′
Region IV (forward)	5′-GACGGCGCGAATAGGGAC-3′
Region IV (reverse)	5′-CTACTATCAGTGACGCTCGTCG-3′
zf5-binding region (forward)	5′-TATTGTGTGGAGCGAGGCAGCT-3′
zf5-binding region (reverse)	5′-GTGTAAACAGTAATAGCGCAGCATGAATTAAC-3″

mRNA. The values (means ± SD) were determined based on results in at least three independent experiments. *P*-values were obtained from Student's *t*-test.

Cell cycle analysis

Cell cycle analysis was performed as described previously (Nanba et al., 2003), using a FACScan instrument (Becton & Dickinson, Franklin Lakes, NJ).

Chromatin immunoprecipitation (ChIP) assay

Mock-treated or EGF-stimulated cells were formaldehyde crosslinked, harvested, and disrupted by Bioruptor (COSMOBIO, Tokyo, Japan), following the method in the EZ ChIP manual (Upstate). Immunoprecipitation was performed with anti-acetylated histone H3 (Upstate), anti-PLZF (Calbiochem, San Diego, CA), or anti-FLAG antibodies (SIGMA). The primers used in this assay are shown in Table 1.

Results

Effect of cell growth factors on proHB-EGF shedding

Shedding of proHB-EGF occurs following stimulation by injury, UV, oxidants, phorbol esters, GPCR agonists, etc. (Takenobu et al., 2003; Higashiyama and Nanba, 2005). To investigate whether stimulation of growth factors such as EGF and bFGF induces shedding of proHB-EGF, we performed an AP-tagged assay with HT1080 cells that were stably transfected with AP-tagged proHB-EGF (Tokumaru et al., 2000). Increasing AP activity in the medium, indicating release of HB-EGF, was detected after stimulation of both EGF and bFGF (Fig. 1A). We also confirmed the production of HB-EGF-CTF after stimulation with these growth factors (Fig. 1B).
A metalloprotease inhibitor, KB-R7785, effectively blocked growth factor-induced proHB-EGF shedding, indicating involvement of metalloproteases in the shedding mechanism, as reported previously (Tokumaru et al., 2000; Nanba et al., 2003; Shirakata et al., 2005) (Fig. 1A). Moreover, we examined the localization of endogenous HB-EGF-CTF in human keratinocytes. Accumulation of endogenous HB-EGF-CTF in nuclei (Nanba et al., 2003) was markedly enhanced by the addition of bFGF, and this was inhibited by KB-R7785 (Fig. 2).

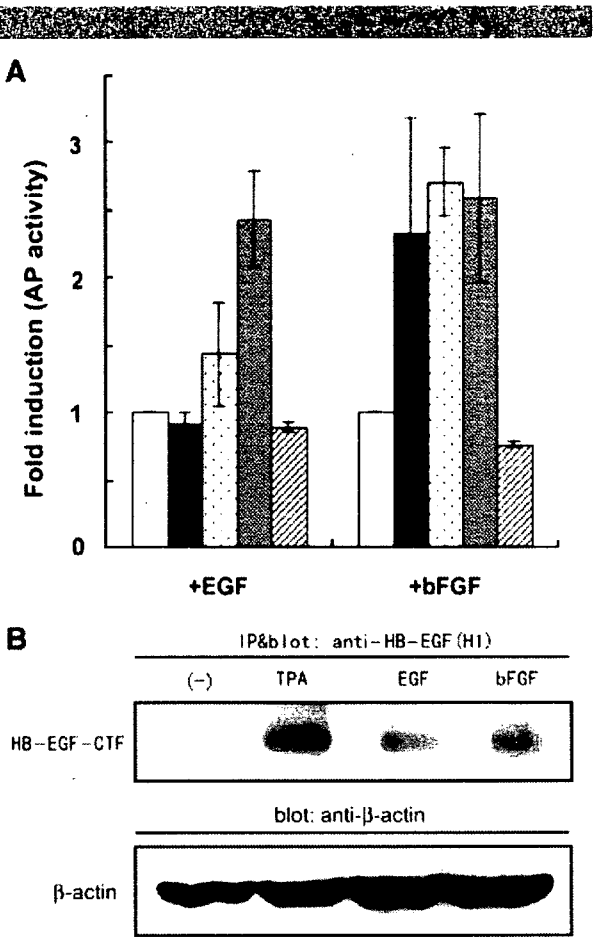

Fig. 1. Induction of proHB-EGF shedding by stimulation of EGF and bFGF. AP-tagged proHB-EGF was stably expressed in HT1080 fibrosarcoma cells. A: These cells were treated with various concentrations of EGF or bFGF for 1 h, and the AP activity was analyzed in each medium. Open bars, no stimulation; closed bars, 1 ng/ml; dotted bars, 10 ng/ml; shaded bars, 50 ng/ml; slashed bars, 50 ng/ml of growth factor and 10 μM of KB-R7785. All experiments were performed independently in triplicate. B: The lysates were collected from the above cells after each stimulation, and immunoprecipitated with anti-HB-EGF-CTF antibodies. After that, SDS-PAGE and immunoblotting with the above antibodies (upper part) were performed. β-actin in each cell lysate was detected with anti-β-actin antibodies as an indicator of protein loading (lower part).

Effects of an inhibitor of proHB-EGF shedding on *c-Myc* expression induced by EGF

We have previously shown that HB-EGF-CTF, which is produced after shedding, regulates the expression of cyclin A2 by inhibition of the PLZF repressor protein (Nanba et al., 2003). PLZF has also been known to inhibit the expression of human *c-Myc* (McConnell et al., 2003). Therefore, we suspected that shedding of proHB-EGF and subsequent production of HB-EGF-CTF may control human *c-Myc* gene expression by abrogation of PLZF function. To examine the involvement of proHB-EGF shedding in EGF-induced *c-Myc* expression, we first performed an RPA with human primary cultured keratinocytes with intrinsic expression of HB-EGF, EGFR, and PLZF. Treatment with KB-R7785, a potent proHB-EGF shedding inhibitor (Asakura et al., 2002), resulted in a decreased expression of *c-Myc* mRNA under growth medium conditions (MDCB153 medium supplemented with insulin and bovine hypothalamic extract) to close to the basal level (Fig. 3A), whereas KB-R7785 did not affect phosphorylation of EGFR and Erk1/2, even when recombinant EGF was present (Fig. 3B). Treatment with a combination of KB-R7785 and anti-EGF receptor antibodies appeared to lead to even greater suppression of the *c-Myc* gene. These results imply that the activation of EGFR signaling brought about full induction of *c-Myc* expression with shedding of proHB-EGF.

To evaluate whether this event is species specific, we also examined expression of *c-Myc* in MEFs. mRNA of *c-Myc* was induced by stimulation of EGF and treatment with KB-R7785 partially suppressed *c-Myc* expression (Fig. 3C), but had no remarkable effect on phosphorylation of EGFR and Erk1/2 under treatment of KB-R7785 in MEFs (Fig. 3D). TPA is one of the strongest inducers of proHB-EGF shedding. To confirm the blocking effect of shedding by the metalloproteases inhibitor, KB-R7785, in MEFs, we performed proHB-EGF-AP shedding assay with adenovirus infection system (Fig. 3E). KB-R7785 even blocked the induction of proHB-EGF shedding by TPA.

Reduction of EGF-induced *c-Myc* gene expression in proHB-EGF-depleted mouse embryonic fibroblasts

To define the transcriptional regulation of *c-Myc* by HB-EGF more precisely, we generated *Hb-egf*-deficient MEFs using Cre/loxP technology (Fig. 4A). MEFs were isolated from loxHB-EGF

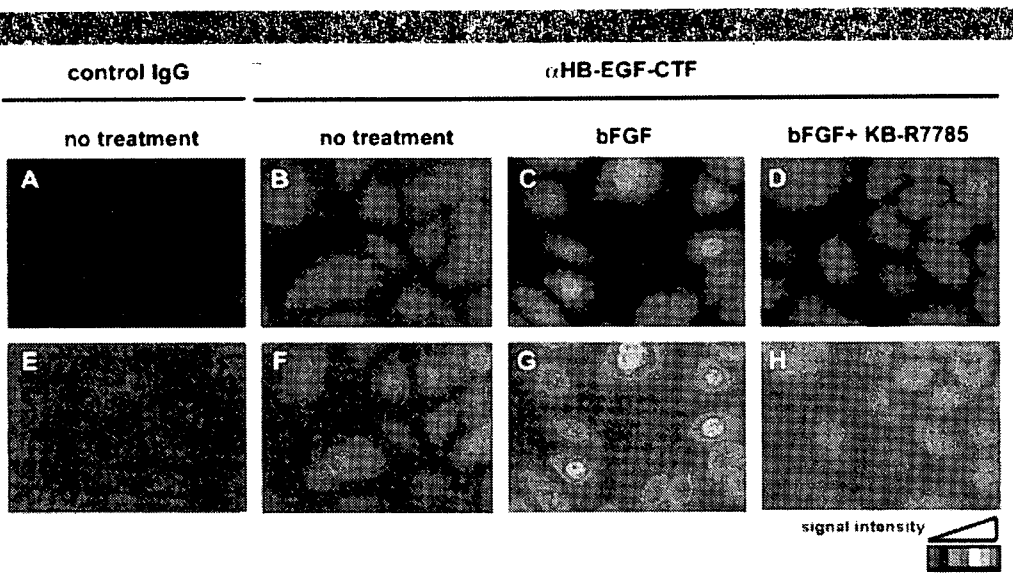

Fig. 2. Intracellular localization of endogenous HB-EGF-CTF in human keratinocytes, determined by fluorescent microscopy. Human keratinocytes were stimulated with 10 ng/ml bFGF for 30 min, after which they were fixed and stained with normal rabbit IgG or anti-HB-EGF-CTF antibodies. A, B, E, and F are images taken before stimulation; (C) and (G) are images collected after stimulation; and (D) and (H) show the effect of KB-R7785 treatment before stimulation with bFGF. A and E, normal rabbit IgG; B–D and F–H, anti-HB-EGF-CTF antibodies. Parts E–H show analytical data for A–D, respectively, determined using Scion Image.

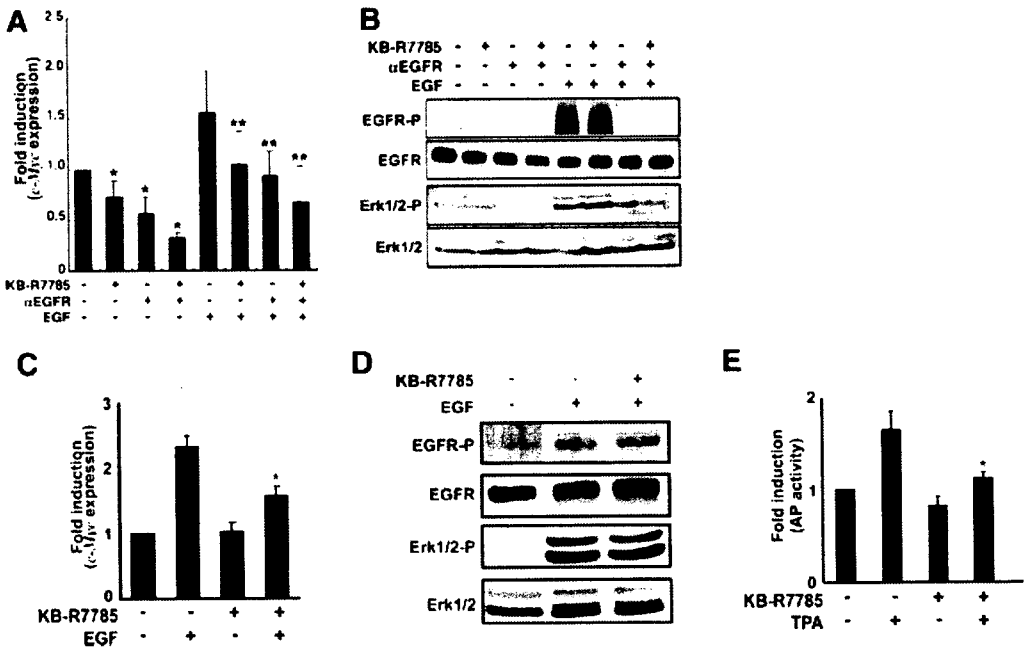

Fig. 3. Involvement of shedding of proHB-EGF in *c-Myc* transcription by human primary cultured keratinocytes and mouse embryonic fibroblasts. A: Analysis of *c-Myc* mRNA expression in keratinocytes by RPA. The intensities of the bands for *c-Myc* and *Gapdh* mRNA were measured by densitometry. In some cases, the keratinocytes were pretreated with 10 μM of KB-R7785 and/or 10 μg/ml of EGFR-neutralizing antibody for 1 h. Some of the cultures were further treated with 10 ng/ml of EGF for 1 h. Expression of *Gapdh* mRNA was examined as a control. $^{*}P < 0.05$ versus non-treated keratinocytes (lane 1) and $^{**}P < 0.05$ versus EGF-treated keratinocytes (lane 5). B: Phosphorylation of EGFR (middle parts) and Erk-1/-2 (lower parts) in keratinocytes was observed in a Western blot assay. C: Analysis of *c-Myc* mRNA expression in MEFs by RPA. The intensities of the bands for *c-Myc* and *Gapdh* mRNA were measured by densitometry. D : Detection of EGF signaling through the EGF receptor by an IP-Western assay. All experiments were performed independently in triplicate. E: Effect of KB-R7785 on shedding of proHB-EGF in MEFs. MEFs transiently expressed with AP-proHB-EGF were stimulated with 100 nM of 12-o-tetradecanoylphorbol-13-acetate (TPA). Before stimulation with TPA, the cells were treated with 20 μM of KB-R7785. $^{*}P < 0.05$ versus EGF-treated MEFs. A and C, The expression level of *c-Myc* was normalized using the level of *Gapdh*, and the fold induction is shown on the basis of the expression ratio relative to no treatment.